Master Thesis

Navigation of ROVs and Basic Signal Processing

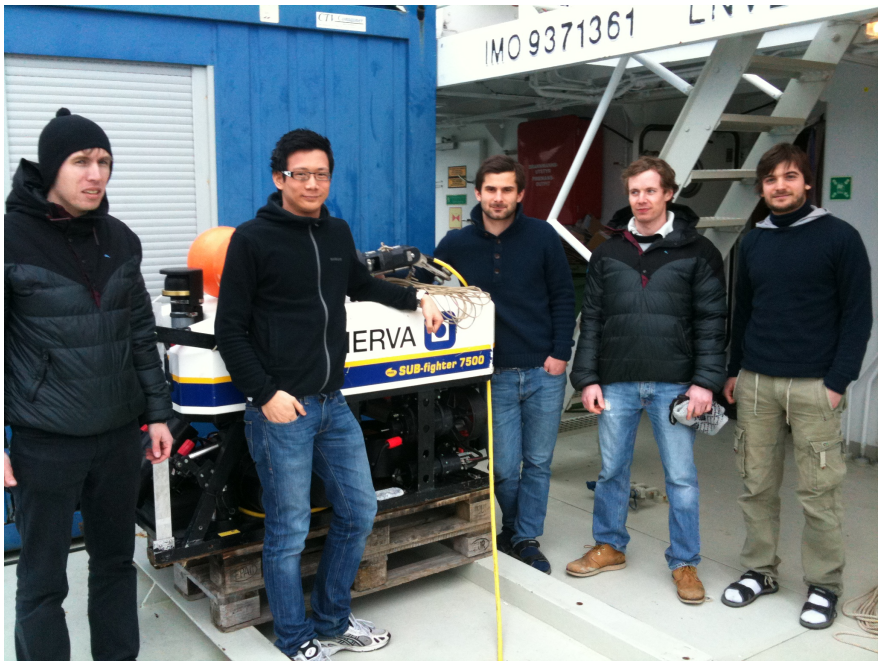

Phat Truong

June 14, 2011

NTNU – Trondheim
Norwegian University of
Science and Technology

Abstract

A dynamic positioning (DP) system for a ROV is being developed in the Automated Underwater Robotics (AUR) laboratory at the Norwegian University of Science and Technology (NTNU). The AUR lab at NTNU has a ROV and a research vessel at disposal for development and testing of the DP system. The DP system is dependent on having a trustworthy and robust navigation system that provides navigational data in order to control the ROV efficiently. Such a system, a navigation computer running a navigation software called Navipac, is currently being provided by a company named EIVA.

It is however desirable to have full control over the raw sensor signals at any given time. The exact details about how Navipac process the raw signals is essentially unknown to the user. A navigation system that will replace Navipac is therefore needed in order to achieve a fully standalone system. This will allow tighter integration with the DP system as well as allowing customizations to fit the DP control system needs.

A navigation system has therefore been implemented using hardware and software solutions provided by National Instruments. The most important functionality of the implemented navigation program is the providing of the needed navigational data to the DP control system. Additional features such as logging utilities for post processing and a graphical user interface (GUI) for easy operation has also been added to the program.

Full scale tests has been performed in the Trondheimsfjord with NTNUs research vessel R/V Gunnerus and ROV Minerva while using the developed navigation system. The tests were successful and the navigation system yielded decent performance. The results however also shows that the performance of the DP system was somewhat degraded compared to when using Navipac for navigation. The degradation in performance was most likely caused by a small delay in the communication between the navigation system and the DP system. Further work should include investigating the cause of this delay closer.

Acknowledgements

First of all, I would like to thank my supervisor, Professor Asgeir J. Sørensen for guidance and advice during the work presented in this thesis. I would also like to thank him for always being positive and encouraging. He is always enthusiastically engaged in his students work and has truly been a source of inspiration for me.

I would also like to thank my co-supervisors, Dr. Martin Ludvigsen and Fredrik Dukan. I would like to thank Martin for helping me understand the hardware and sensor configuration and specification in detail and for always being available on the phone when technical assistance is needed during operations with the ROV Minerva. I would like to thank Fredrik for helping me and providing advice during the implementation of the navigation system. He has helped my understanding of Labview coding as well as helping me getting started by providing code for me to modify and further develop.

Further, I would like to thank the others that has been involved in this project; Daniel de Almeida Fernandez, Laura Standardi and Mauro Candeloro for being a good team and for supporting each other. I would also like to thank fellow master student Steffen Kørte for the exchange of ideas, feedback and general advice in life.

Lastly, I would like to thank the wonderful crew on R/V Gunnerus; Arve, Sven Ove, Steinar and Mads. I would like to thank them for always being in a good mood and for providing a proper meal at least once a moth. I would also like to thank Robert Staven for showing me how to set up the ROV Minerva for testing on land.

Phat Truong
13. June 2011

Contents

List of Figures

List of Tables

Chapter 1

Introduction

This thesis is a continuance from previous work done in the fall of 2010, where a pre study of navigation principles and system configuration was made along with post processing of navigational data. A Dynamic Positioning (DP) system is currently being developed for the Norwegian University of Science and Technology (NTNU) Remotely Operated Vehicle (ROV) Minerva in conjunction with the Applied Underwater Robotics (AUR) lab at NTNU. In order to ensure fluent and safe navigation of the ROV, a navigation module handling the raw data from the sensors should be developed alongside the DP system. This navigation module should handle the kinematics of the sensor placements and signals as well as signal processing of the raw data transmitted from the different sensors. There are many areas of concern when dealing with this matter, e.g. signal validation, measurement noise, disturbances, timing principles and signal logistics to mention a few. If a navigation system is going to be made from the ground up, there are also hardware related challenges that arise. Choice of hardware interface and software platform will greatly affect the task. The objective of this thesis is to create such a navigation system that is going to be used with the control system when operating the ROV Minerva.

1.1 Background and Motivation

Unmanned underwater vehicles (UUVs) are being used for numerous purposes worldwide, ranging from industrial operations and maintenance to research operations and science surveys. Unmanned underwater vehicles are divided into two types, ROVs and UAVs. A ROV (Remotely Operated Vehicle) differs from an AUV (Autonomous Underwater Vehicle) in the sense that it is connected to a tethering vessel or some operational station by a physical cable. The tether cable provides energy for the ROV as well as communication between the ROV and the operation station. An AUV on the other hand, carries its own power system and has its own control system for autonomous operation and navigation.

The ROVs and AUVs have different attributes when it comes to performance and capabilities. The ROV is usually fully actuated whereas the AUV is typically underactuated. The extended communication possibilities between the ROV and the operation station makes it more suitable for mechanical work. The AUVs on the other hand are more hydrodynamical constructed and are designed to operate

without any input from the operator.

ROVs are often utilized in subsea operations in the gas and oil industry. These operations can range from monitoring to maintenance and installation of subsea structures. ROVs can be equipped with tools and/or hydraulic arms that can ensure its capability to perform certain tasks. Precise navigation is therefore extremely crucial during these operations, as a simple drift of as little as a few meters can cause damage that can result in enormous consequences. ROVs are also used extensively for scientific purposes. The Trondheim Biological Station (TBS) frequently use the ROV Minerva to collect biological samples, exploration of the seabed and monitoring of fish in conjunction with different biological studies. AUVs on the other hand are mostly used for seabed investigation and surveys. Commercial use of AUVs include detailed investigation of the seabed during planning of subsea installations, pipeline constructions or drilling operations. The military use AUVs to detect and locate mines on the seabed. AUVs are also used in research to study lakes as well as the ocean floor.

A navigation system called Navipac made by EIVA is being used during operations with the Minerva today. A motivation to replace Navipac is to obtain a fully standalone system where everything is handled from the raw sensor measurements to desired thruster forces. By designing a new system, the navigation software can also be designed to interact with the control system more extensively than before. It is desirable to have full control over all the sensor signals at any given time, as opposed to relying on a third party where the detailed processing of the signals is essentially unknown and the control loop will contain a so called *blackbox*. The development of a new navigation system will also create an exciting field of exploration and work for future students in connection with the AUR lab.

1.2 Previous Work

1.2.1 UUVs

The *Norwegian Defense Research Establishment* has in collaboration with *Kongsberg Simrad* developed the *HUGIN* family of autonomous underwater vehicles. These AUVs have been used extensively in commercial survey operations. The Norwegian Defense Research Establishment and Kongsberg Simrad has developed a integrated inertial navigation system for their HUGIN range of AUVs. Their Inertial Navigation System (INS) calculates position based on Inertial Measurement Units (IMU). The INS is aided by non inertial instruments and combined in a error state based Kalman filter to optimize the navigational performance, Jalving et al. [2004].

(a) Hugin 1000. (b) Remus 6000.

Figure 1.1: AUVs. Photos: Kongsberg Maritime.

Kongsberg Hydroid has also developed a family of AUV products for Kongsberg Maritime called *Remus*. The sensors that these AUVs are equipped with are Doppler Velocity Logs (DVLs), GPS, INS, sonars, conductivity & temperature sensors and pressure gauges. In addition, optional instruments such as acoustic imaging and video cameras, are available if desirable. Earlier this year the remains of the Air France passenger airplane that crashed in the Atlantic Ocean June 2009 was found using a couple of Remus 6000 AUVs.

Figure 1.2: Flight recorder of Air France wreckage recovered at 4000 m depth. Photo: Bureau of Investigation and Analysis.

1.2.2 Navigation Systems

Kearfott Guidance & Navigation Corp has developed an integrated INS/Global Positioning System (GPS) called *SEANAV*, Beiter et al. [1998]. The SEANAV system is based on the same aiding principle as the navigation system for the HUGIN AUVs, using IMUs and non inertial instruments combined in a Kalman filter to optimize the navigation performance.

The Norwegian Defense Research Establishment has also developed a simulation and post processing tool for research and development, analysis and real data post processing called *NavLab*. NavLab is based on the *Matlab* environment and is intended to be used to test and improve new navigation system designs, Gade [2004]. Navlab consist of two parts, a simulator and an estimator. The simulator can be used to simulate real sensors in order to test a navigation systems performance. The estimator calculates an optimal estimate of the position, velocity and orientation of a vehicle using either real or simulated sensors and can be useful to evaluate the robustness of a given sensor configuration.

Kongsberg Maritime has developed a navigation system for AUVs and ROVs called *HAIN* (Hydroacoustic Aided Inertial Navigation). As the name suggests, HAIN is a combination of acoustic and inertial positioning system. The principle is the same as in GPS aided INS systems. The drift of the INS is corrected by the hydroacoustic positioning system.

1.3 Contributions

The contributions of this thesis are:

- A foundation has been made in the development of a navigation system. The sensor logistics has been handled as well as the interpretation of the raw formats from the various sensors. Logging applications has been made in order to post process the signals and states of the system. Future developers of the navigation system should be able to fully concentrate on the signal processing and estimation of states.
- Kinematics of the sensor configuration has been handled. An effort has been made to identify the exact offsets of the vessel sensors.
- A simple Kalman filter has been implemented with possibilities of extension to include additional states in the case of an addition of a inertial measurement unit. The performance of the filter should however be improved in the future.

1.4 Outline

Chapter 2 will give a brief overview of the ROV and vessel specification and sensor configuration.

Chapter 3, 4 and 5 will present the main concept and means of navigation that are available today.

Chapter 6 will explain the basic kinematics and transformation between different reference frames. An overview of map projections as well as ellipsoidal earth models will be presented.

Chapter 7 will explain the Kalman filter equations.

Chapter 8 will describe the navigation system that has been implemented in detail as well as hardware configuration and setup of the system.

Chapter 9 will present the result from full scale testing and comparison between the performance of the implemented navigation system and the third party navigation system Navipac.

Chapter 2

System Specification

The AUR lab at NTNU currently has a research vessel and a ROV at disposal. R/V Gunnerus is a research vessel that is owned by NTNU, and it is available for the AUR lab to use upon agreement. The R/V Gunnerus is mainly being used to do a variety of research activities within biology, technology, geology, archeology, oceanography and fisheries research. It was specially designed to have low hydroacoustic noise levels to accommodate testing and development of hydroacoustic equipment. It is also fitted with a wet lab, a dry lab and a computer lab. The R/V Gunnerus was built by Larsnes Mekaniske Verksted in Norway and was delivered in 2006. It was named after Johan Ernst Gunnerus(1718-1773) who was a scientist within bothany and zoology, bishop in Trondheim and one of the founders of Det Kongelige Norske Videnskapers Selskap, NTNU. [2010]. The vessel is equipped with a DP system and a HiPAP unit, which makes it able to position any deployed unit by attaching a transponder to this unit. This makes the R/V Gunnerus optimal for e.g. ROV operations. It has a personnel capacity of 25 people including the crew.

(a) R/V Gunnerus starboard side view. Photo: Fredrik Skoglund. (b) ROV Minerva. Photo: Johanna Järnegren.

The ROV Minerva is a SUB-fighter 7500 made by Sperre AS for NTNU. Minerva was specially designed by Sperre to meet the requirements of scientists at NTNU. It is mainly being used to do research, archaeological studies, geological investigations and collect biological samples among other things. It is also being used to test and develop new research technology and it is a useful tool in many courses at NTNU.

2.1 Specifications for R/V Gunnerus

(c) ROV operation. Photo: Ø. Lamo.

(d) Engine room. Photo: T. Magelssen.

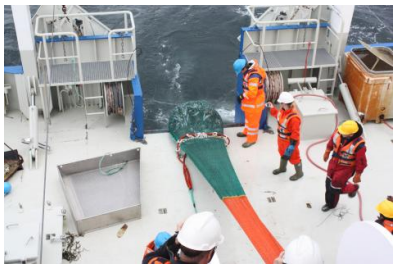

(e) Trawling. Photo: A. Knudsen.

Figure 2.1 lists the main dimensions of the R/V Gunnerus. The vessel is equipped with two diesel electric propulsion engines made by Siemens with an effect of 500 kW each. The diesel electric system has been specially designed to produce very low hydroacoustic noise levels in order to optimize performance hydroacoustic instruments. The top speed of the vessel is 12.6 knots while the cruise speed is 9.4 knots. The vessel is equipped with a range of instruments including multi beam echo sounders and motion reference units (MRU). The sensors on the vessel that are of importance when making a navigation system for the ROV Minerva is the Furuno GPS, Kongsberg Seapath 300 and the Kongsberg HiPAP 500. The details about these sensors are given in Table 2.1.

Description	**Size**
Overall length	31.25 m
Length in waterline	28.9 m
Width middle	9.6 m
Width extreme	9.9 m
Depth of main deck	4.2 m
Draught	2.7 m
Weight	107 tonns

Figure 2.1: Main dimensions of R/V Gunnerus.

Instrument	**Description**	**Uni**	**Resolution**	**Offset relative to the vessels center of origin (x,y,z)**	**Data transfer**	**Update rate**
Furuno GPS	Ellipsoidal north and east position	Longitude, latitude and height	0,01	(10,1,8)	UDP Port 3001	10hz
Kongsberg HiPAP 500	Position in vessel body frame	m	0,01	(0,0,0,)	UDP Port 1004	ca 0.5-1 hz [1]
Kongsberg Seapath	Heading, attitude and position (used only for heading)	deg	0.1	-	UDP Port 3002	10hz

Table 2.1: Gunnerus sensor specifications.

2.2 Specifications for Minerva

The ROV Minerva measures 1,44[m] long, 0,82[m] wide and 0,80[m] high. It weighs 405[kg] and is capable of handling payloads up to approximate 20[kg]. It is equipped with five 1500[W] thrusters, two horizontal, two vertical and one in lateral position. It is capable of operating in depths up to 700[m] and is equipped with two cameras and a hydraulic arm that enables it to perform seabed investigations. Minerva is also equipped with a sonar that can be used to map the terrain of the seabed. Minerva is operated from a customized cargo container which houses the necessary equipment including a 42 inch flat screen capable of showing real time video footage from the ROV.

The sensors that are needed for navigation of the ROV is listed in Table 2.2 as well as the relevant specifications.

Instrument	Description	Unit	Resolution	Update rate	Data transfer
ADCP	Surge/Sway speed	m/s	0,01	10 hz	RS232 Port
Compass	Heading	deg	1	10 hz	RS232 Port
Gyro	Yaw rate	deg/s	-	10 hz	RS232 Port
Pressure gauge	Depth	m	0,1	10 hz	RS232 Port
Sonar	Altitude	m	0,1	10 hz	RS232 Port

Table 2.2: ROV sensor data

2.3 System Setup

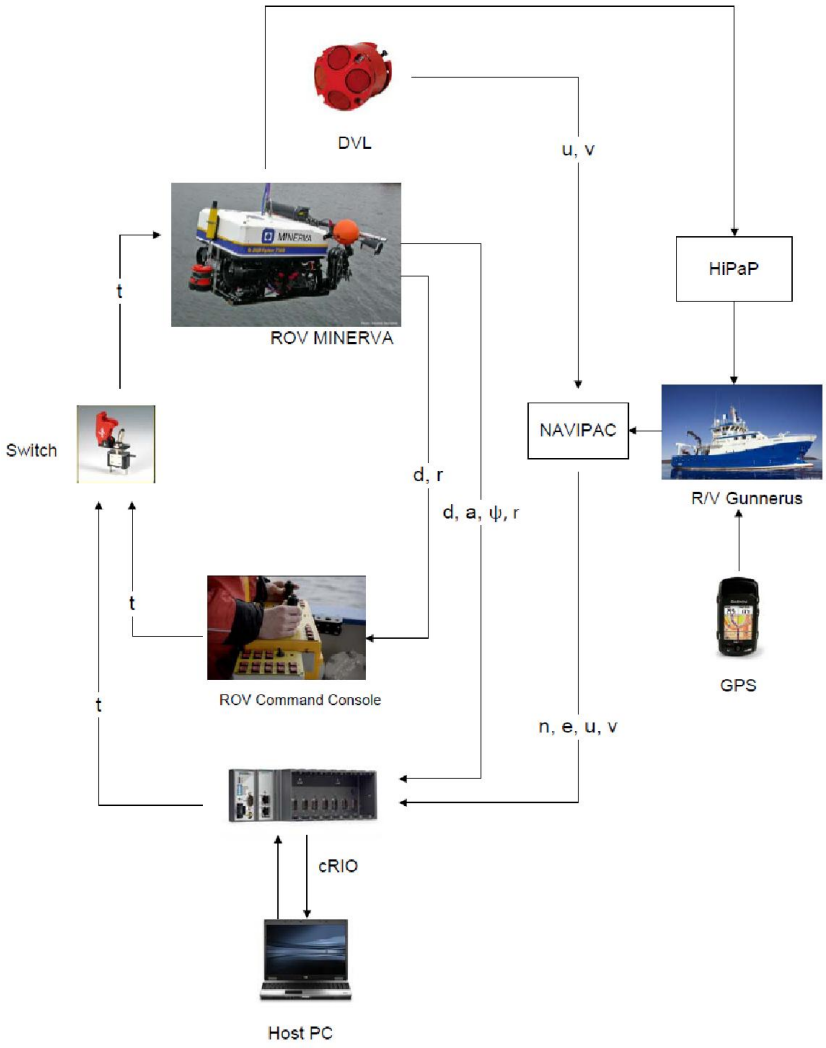

Figure 2.2: Signal flow of the control system. Illustration: Fredrik Dukan.

R/V Gunnerus and the ROV Minerva are equipped with numerous instruments to acheive accurate position. The setup of the control system and signal flow is illustrated in 2.2. The Navipac module receives the raw sensor data from the GPS and HiPAP on the vessel and the raw data from the Doppler Velocity Log (DVL). Navipac calculates the ROV position and filter out measurement noise through a Kalman filter. The control system, consisting of a National Instruments Compact RIO (cRIO) module and a host PC, receives the filtered signals from Navipac in addition to raw signals from the compass, gyro, sonar and pressure gauge on the ROV. The control system then outputs the commanded thrust to the ROV. The system is also equipped with a manual control mode where a human operator can control the ROV using a console. Transition between the control system and manual control mode can be toggled by a switch.

Chapter 3

Global Navigation Satellite Systems

Global Navigation Satellite Systems (GNSS) are satellite based radio navigation systems that can provide information about position and velocity of a receiver. After the launch of the first satellite, the russian *Sputnik 1* in 1957, engineers discovered that the position of the satellite could be calculated by the doppler shift of the signal transmitted from the satellite to a receiver with a known location. This solution is still valid in the reverse case where the satellite position is known while the position of the receiver is unknown. The development of satellite based navigation systems soon followed. Although the first intended use was for military purposes, the first satellite navigation system, *Transit* (or NAVSAT) developed by the US military in 1964, was broadly used for navigation after the system became available for civilians in 1967, Kjerstad [2010].

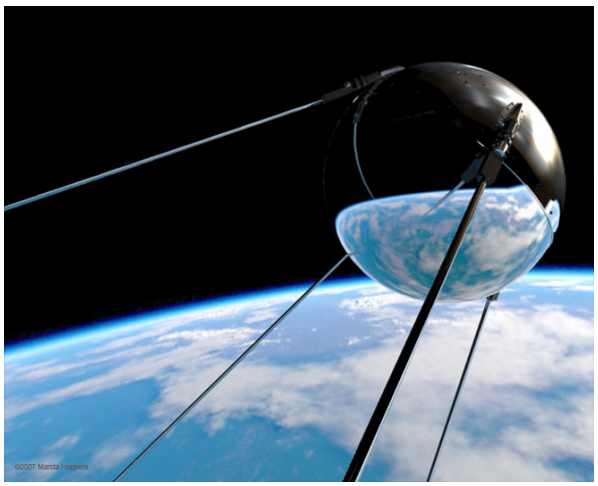

Figure 3.1: Sputnik 1 in orbit. Photo: Marcia Hoppers.

The satellites that was used in the first navigation systems travelled around the Earth in an elliptical *low Earth orbit (LEO, between 160-2000 km)*. Because of the LEO of the satellites, continuos positioning by the system was limited by the geometry of the satellite positions. The doppler based systems also suffered from inexact positioning when the velocity of the receiver was unknown. These drawbacks of the old system lead to the development of the technology that is used today in GNSSs. In order

to cover larger geographical areas, the satellites were launched into a *medium Earth orbit (MEO, between 2000-35786 km)* and atomic clocks enabled the system to deduce the position by measuring time instead of the doppler shift of the signal.

Currently there are four big GNSSs that are either complete or under development; GPS, GLONASS, GALILEO and COMPASS. The systems are American, Russian, European and Chinese initiatives respectively.

3.1 Global Positioning System

The first operational Global Positioning System (GPS) satellite was launched in 1978 and the system was complete and fully operational in 1994. The constellation of satellites today consist of 30 operational satellites that are placed in 6 orbital planes with an inclination of 55° between each plane, see Figure 3.2. The choice of inclination angle and number of satellites in this constellation ensures that at least five satellites always will be visible for a receiver from any point in the world.

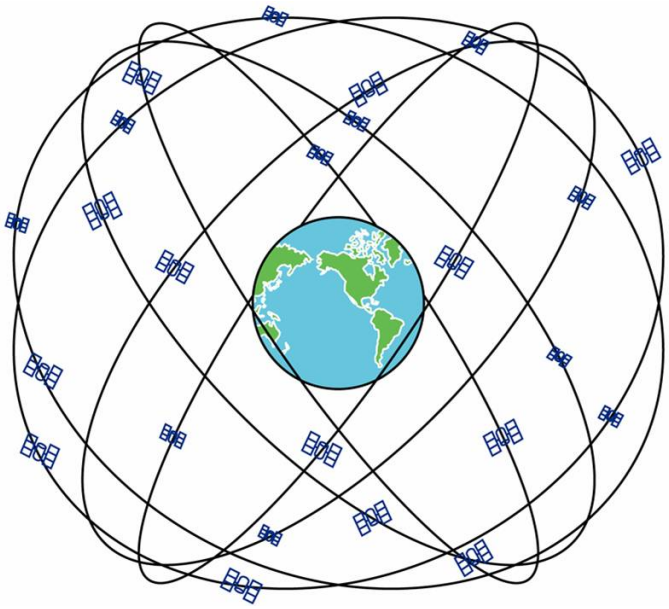

Figure 3.2: GPS Constellation. Illustraton: Digital Earth Research Center.

The precision of the GPS system can range from *millimeters* to *meters* depending on the positioning method and the observable. The distance from satellite to receiver can be determined by observing either the *code phase* or the *carrier phase observables* . The most extensive use of GPS today, as seen in consumer level receivers, use the code phase to determine the position. This usually gives an accuracy in the range of 2-5 meters. In addition to regular positioning there is a enhanced mode of positioning called *Differential GPS, (DGPS)*, where a reference station with a fixed and known position is used to estimate the errors. This will result in an accuracy in the range of 1-2 meters. Using the carrier phase observables to determine the distance on the other hand, requires more advance equipment. In addition the carrier phase observables are much more postponed to ambiguities and

multi-path interference. There are two positioning methods when using the carrier phase observables. The most accurate method is a post processing method called *Baseline GPS* which utilizes two fixed and known positions and the measured distance (the baseline) between these positions to determine the system errors. This will result in an accuracy of 1-2 millimeters. The second method is called *Real Time Kinematic (RTK)* which utilizes a base station with a fixed and known position. A special receiver is used and in addition the distance between this receiver and the base station is measured accurately. This distance will serve as a real time baseline that is used to calculate the errors. This method will give an accuracy in the range of 1-2 centimeters.

3.1.1 Basic Concept of Positioning

A GPS receiver measures the time from when a signal is sent from the satellite until the signal reaches the receiver. From this time measurement, the distance between the receiver and the satellite can be calculated by multiplying with the speed of light, as the signal sent from the satellites propagates with this speed. The distance between the satellite and the receiver that is obtained is called a *pseoudorange*. This is due to the fact that this distance will contain an error because of some clock bias depending on the quality and precision of the clock of the receiver. The satellites however, are equipped with the most precise clocks that have been developed; the atomic clocks. In order to determine the position of a receiver in three dimensions, a minimum of four satellites is required in order to obtain a solution. Theoretically, only three satellites is needed, but because of the clock error a fourth satellite is needed to account for propagating error.

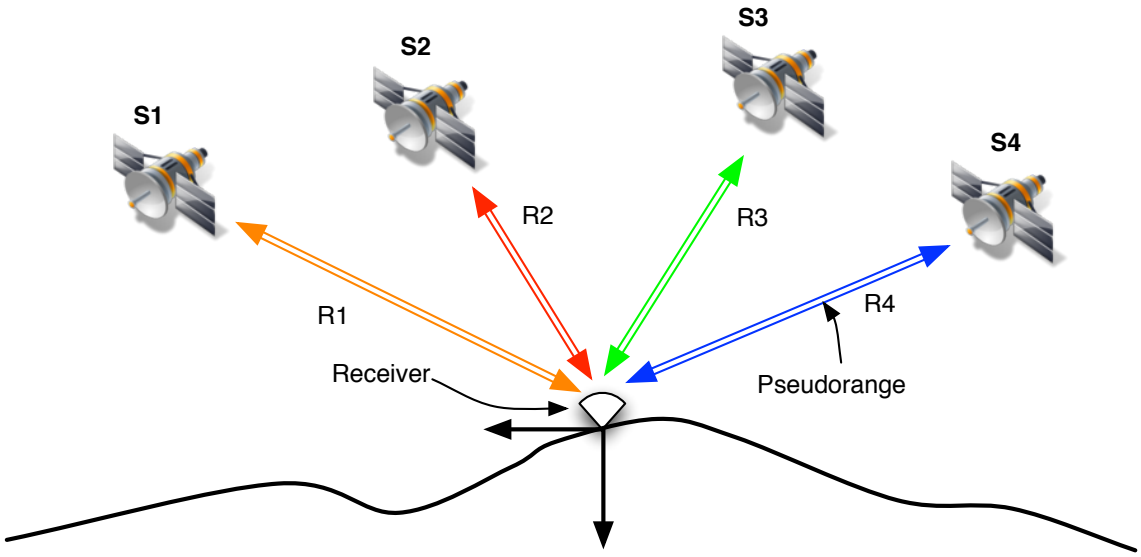

Figure 3.3: GPS positioning scenario.

Once the pseudoranges have been determined, the position of the receiver can be calculated geometrically using the known positions of the satellites. Calculation details can be found in Forssell [1991].

3.1.2 System Architecture

GPS is in general divided in to three segments; a space segment, a user segment and a control segment.

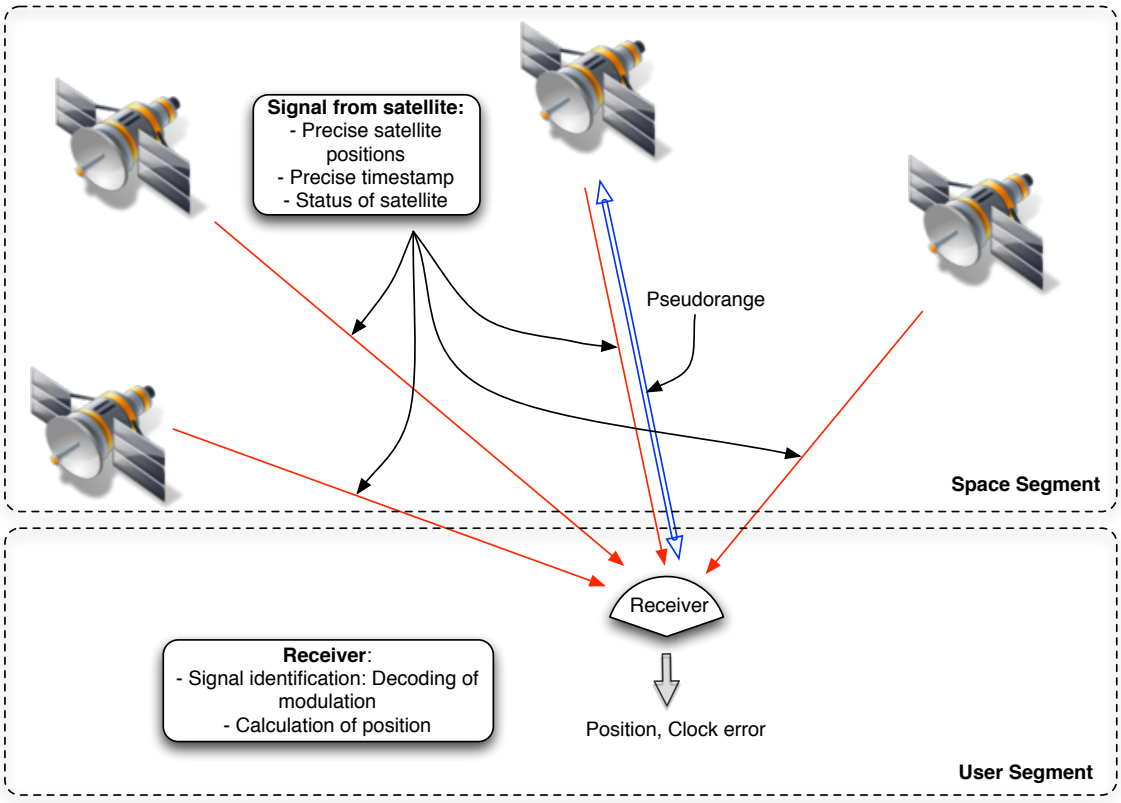

Figure 3.4: GPS. Interaction between space segment and user segment.

Space Segment

GPS is a *passive* system. This means that there is only oneway communication between the satellites and the receiver. All the satellites transmits signals on the same frequenciy bands: L1=1572.42 MHz, L2=1227.60 MHz and L5=1176.45 MHz. In order for the receivers to differentiate between the satellites, a code divided chanelling (CDMA) is used. In short, this means that each of the satellite signals are modulated with a unique *PRN-code* that has to be identified and decoded by the receiver. All the satellites transmits a continuous signal which contains precise information about:

Satellite Position: The satellite always has updated information about its whereabouts on the elliptical orbit. This information is crucial in order for the receiver to calculate its position. The satellite position information is called the *broadcast ephemeris*. In different GNSS the format of the ephemeris may vary.

Timestamp of Signal: All the satellites within a GNSS have synchronized clocks. The clocks that are used on the satellites are atomic clock which are very precise clocks. Because these clocks are expensive, consumer end receivers usually have cheaper and less precise clocks that will lead to clock errors.

Status of the Satellite: The general health of the satellite and an overview of the approximate location of all the other satellites in the constellation is also broadcasted.

User Segment

Because the satellites are transmitting data continuously at the same time on the same frequency, the receiver has to identify each satellite. When the satellite signals are transmitted on the same frequency band, the signals have to be modulated with a unique code, a *PRN-code*, on each satellite in order for the receiver to distinguish between the satellites. The modulation of the satellite signals is an extensive subject and will not be explained in detail. Details are referred to Forssell [1991]

Control Segment

The control segment consist of a main command central situated in the Colorado Springs in the USA, in addition to several monitor and satellite control stations scattered all over the world. The main command central monitors the whole satellite constellation by the use of monitor stations. In order for the satellites to provide precise information to a receiver about its location, the satellite has to receive this information from the command central by the use of ground antennas.

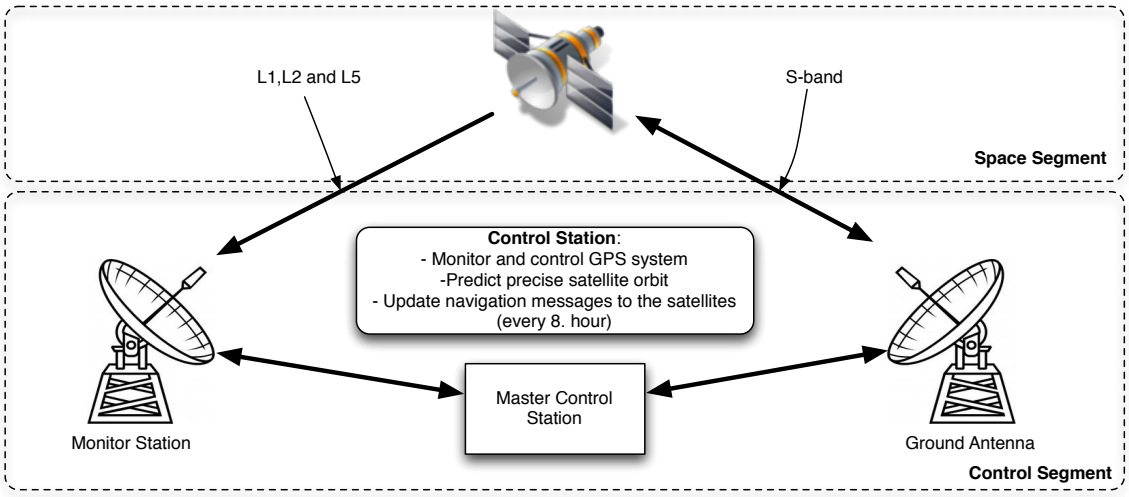

Figure 3.5: GPS. Interaction between space segment and control segment.

3.2 Other Global Navigation Satellite Systems

Although GPS is the only fully functional system to date, there are several independent GNSS initiatives by Russia, China and European countries under development.

3.2.1 GLONASS

GLONASS (Global'naya Navigatsionnaya Sputnikovaya Sistema) is a russian GNSSs that is very similar to the american GPS. The development of this system was started in 1976 and the first satellite was deployed in 1982 and the system has currently 23 operational satellites. The complete constellation will consist of 24 satellites with an inclination of 65.8° and the last satellite, that is currently in an commissioning phase, is scheduled to be fully operational within the end of 2011, Federal Space Agency [2010]

GLONASS is very similar to GPS in principle, but the fundamental differences between the systems is the signal itself and the structure of the signals. GPS satellites transmit signals on the same frequency and use code division channeling (CDMA) to separate the satellites (FDMA). GLONASS on the other hand uses frequency division channeling to separate the satellite signals. The mathematical models that are used to predict the satellite positions are also different from GPS. GPS uses Kepler elements to describe the satellite position while GLONASS describes the satellite position using cartesian coordinates which is reflected in the broadcast ephemeris sent from both systems. Using Kepler elements to describe the satellite positions versus cartesian coordinates will demand a slower frequency of updating the satellite data from the master control station (every 4. hour for GPS and every 15 minutes for GLONASS). The tradeoff however, will be the computational demand needed to calculate the position on the receiver side.

3.2.2 GALILEO

GALILEO is a GNSS project currently under development by the European Union (EU) and the European Space Agency (ESA). The system has currently two test satellites in orbit and the planned constellation will consist of 30 satellites where 3 satellites will serve as active backups. The satellites will travel in MEO height and with an inclination angle of 54° between each of the planes. Specific details about the system has not yet been fully decided, but the purposes of the system will serve civilian causes as opposed to GPS and GLONASS which primarily was developed with serving military purposes in mind and then later on has extended its availability to civilians.

GALILEO is planning to perform open access services to the mass markets, controlled access services with higher precision that requires access, safety of life services and search and rescue services with the possibility of two way comminication between system and user. GALILEO has no official date of completion, but press releases suggests that the system will be operational by early 2014, Commons [2011].

3.2.3 COMPASS

COMPASS is a GNSS that is under development by China and the planned constellation will consist of 27 satellites in a MEO. The first satellites were launched in 2007 and the system is planned to be fully operational sometime between 2016-2020, Kjerstad [2010]. The system mode of operation will in principle be the same as GPS and the same goes for performance and use of frequency.

3.3 Disturbances and Error Sources

Satellite navigation systems are exposed to a variety of error sources and disturbances. The main disturbances and error sources are:

Prediction of Satellite Orbit: Uncertainty and unreliability of satellite orbit parameters can result in inaccurate positioning.

Ionospheric and Tropospheric Disturbances: When the signal is traveling through the Ionosphere and the Troposphere, it may be subjected to deflection.

Dilution of Precision: Poor geometric conditions can cause inaccuracies in position.

Multi-path Reflections: Reflection of the signal can disturb the receiver.

Clock errors and Receiver Noise: Clock error in the receiver and the receiver noise can also cause loss of precision and loss of signal.

Chapter 4

Underwater Navigation

Underwater positioning instruments today mostly rely on the principle of underwater acoustics. This means that most of the methods and techniques that are used utilizes sound to gather the information needed for the intended purpose. Instruments such as echo sounding beams, sonars, hydroacoustic positioning systems and doppler velocity logs are the most widely used sensors commercially. Although underwater instrumentation is mostly based on hydroacoustics, there also exists instruments that are based on the application of light in water, for example laser bathymetry, Kjerstad [2010]. The main principles behind these types of instruments will be explained. A brief overview of hydroacoustic principles and phenomenas will also be presented.

4.1 Hydroacoustics

Hydroacoustics is the study of sound in water. The reason why the application of sound is used for underwater navigation is because sound is less subjected to damping versus electromagnetic waves and light when traveling through high density mediums such as water. The application of sound in water also has a lot of aspects that needs to be taken into consideration when developing accurate hydroacoustic instruments.

Speed of sound

The speed of sound varies with the density of the medium in which it travels in. The speed of sound in water is $c = 1500m$, Kjerstad [2010]. In addition, temperature and pressure also affects the speed of sound. Variables such as depth, salinity and temperature must be included in order to calculate the speed of sound more precisely. An example of an empirical formula for the speed of sound can be written as, Kjerstad [2010]

$$c = 1448.6 + 4.618t - 0.0523t^2 + 1.25(S - 35) + 0.017D \tag{4.1}$$

where t is the temperature ($^\circ C$), S is the salinity (‰) and D is the depth (m).

Curvature

Because the sound in water varies as explained above, the path of the sound is subjected to curvature. It is common to use a velocity profile, which describes the speed of sound as a function of depth in order to calculate the curvature of the sound path. These velocity profiles can be obtained by the use of Conductivity, Temperature and Depth (CTD) sensors which measures temperature, conductivity and pressure from surface to sea bottom.

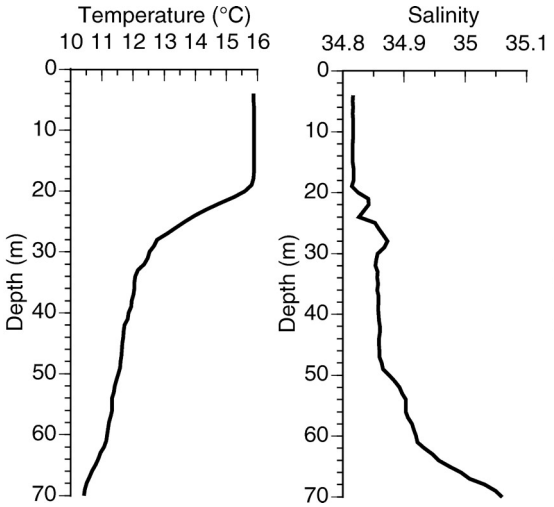

(a) Measurements taken at Fastnet Rock, outside of Ireland. Plot:Kristin E. Gribble and Anderson [2007].

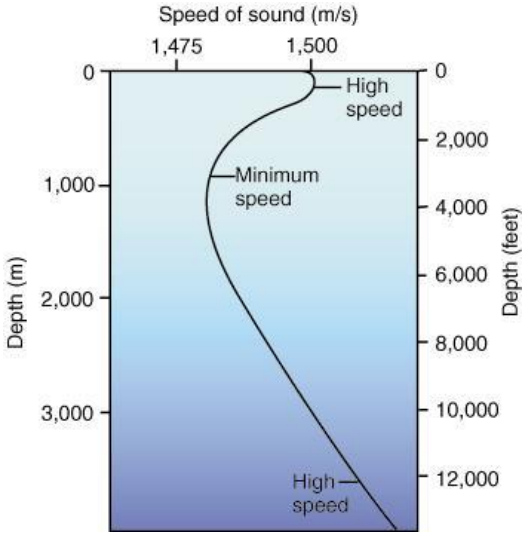

(b) Sound speed in water. Plot: Puna Ridge.

If the gradient, g, of the velocity profile is constant, the path of the sound will follow a circular bow with a radius R. The path will therefore depend on the angle of the transducer from which the sound pulses are transmitted, θ, relative to the horizontal plane and the gradient of the velocity profile, c, as a function of depth, D. The radius can be expressed as, Kjerstad [2010]

$$R = -\frac{c(D)}{\cos\theta}\frac{1}{g}. \tag{4.2}$$

Absorption

When sound travels through water, the energy of the acoustic waves will be absorbed by the water and transformed to heat. The longer the sound waves travels through the water, the more energy is being absorbed. The intensity of the signal is inverse proportional with a factor A and the loss of intensity will increase exponentially with the distance travelled. The intensity can be written as, Kjerstad [2010]

$$\Delta I = -AI\Delta R, \tag{4.3}$$

where ΔI is the difference in distance, ΔI is the difference in intensity of the signal and A is the frequency dependent absorption factor.

Acoustic Shadows

Acoustic shadows are areas where a signal is not received, or when a signal is received in a place where it should not have been any signal. This phenomena can be the result from several causes. The main causes are curvature of the acoustic sound waves, damping of signal, masking of signal and echoes from side of the transmitter beam.

Noise

In the ocean there are many acoustic sources that can interfere with hydroacoustic instrumentation, Kjerstad [2010].

- **Noise from waves and wind**: Waves and wind will generate low frequency noise. The magnitude will depend on the sea state, but even at calm seas the waves and wind will have a given noise level.
- **Thermal noise**: The movement of molecules in water particles will cause thermal noise. The effects of thermal noise will impact the higher frequencies and starts to dominate above 100 kHz.
- **Vessel generated noise**: Vessel generated noise can come from the instruments own ship or nearby vessels. The main source of noise is the propeller. On large vessel the with big propellers, the noise can be very intensive. In areas carrying a great deal of traffic, the background noise will be dominated by vessel generated noise. In addition to the propellers, noise can be caused by other rotating machinery on board a vessel, like rotational speed of the engines and gear shifting.
- **Acoustic interference**: In the case where several ships are in the same geographical area and have sonars that operate in the same frequency range, the sonars may interfere with each other. The interference will appear as occasional false echoes and the range at which these interferences may be experienced can vary from a few nautical miles to several hundred nautical miles.
- **Biological noise**: Some underwater creatures communicate with sound that can interfere with the instruments. Although these disturbances are not critical for most applications of underwater instrumentations, they are nevertheless intercepted by the transponders.
- **Receiver noise**: Receiver noise can be characterized as white noise that is evenly spread across the whole spectrum. In order for the receiver to register a signal, the received signal must have higher energy than the noise level of the receiver. This is commonly described by the use of a *signal to noise ratio* (SNR=signal/noise).

4.2 Echo Sounder

One of the first underwater navigation instruments that was developed for commercial use was the single beam echo sounder. The single beam echo sounder measures the time it takes to receive a reflection from a ping that is sent from the transducer. By comparing the frequency of the sent signal and the received signal, the distance from the transducer to the object that is reflecting the signal can be calculated. The single beam echo sounder is used today to as a simple depth measurement device on larger ships. Echo sounding is also widely used by fishing vessels to locate larger schools of fish underneath the surface in addition to detailed bathymetry surveys for scientific purposes.

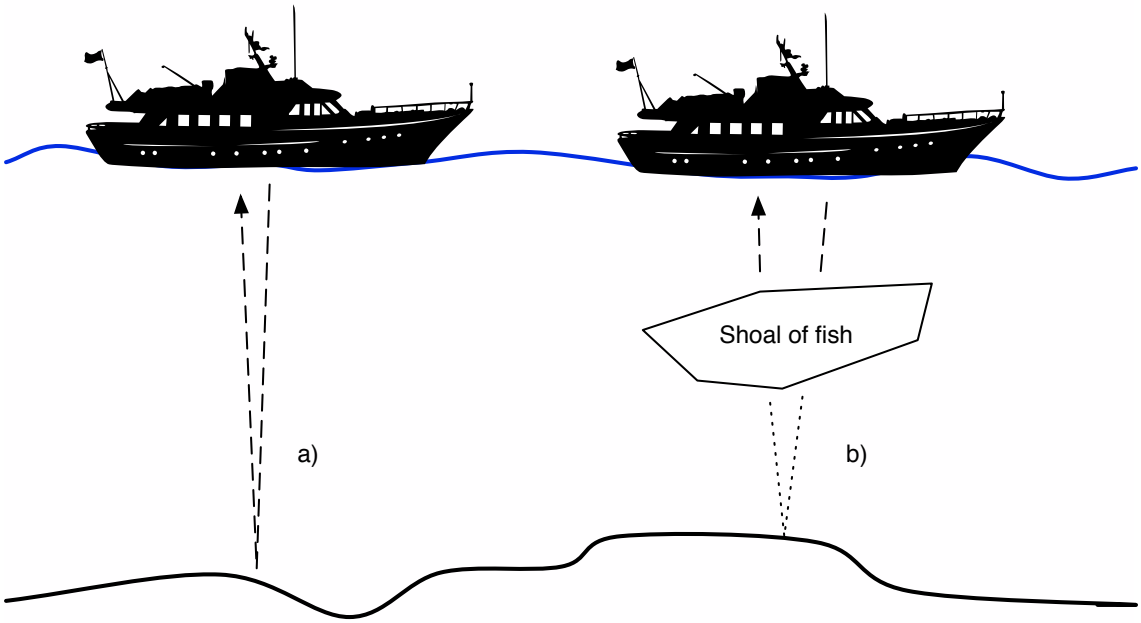

Figure 4.1: Echo sounding scenarios.

The accuracy of an echo sounder will vary with the water properties. If higher accuracy is needed, an appropriate sensor can be lowered into the water to measure salinity, temperature and pressure. Using these measured variables, the speed of sound in water can be calculated more precisely in accordance to the situation and conditions.

4.2.1 Multibeam Echo Sounder

The multibeam echo sounder can be described as something between a single beam echo sounder and a sonar. A multibeam echo sounder will usually have between 3-5 beams that are either fixed relative to each other or configurable by the operator. Each beam works just like the single beam echo sounder as described above. The configuration of the beam positions may be chosen according to the intended operation. Multibeam echo sounders have the ability to detect an obstacles position along the beam as well as the approximate size of the object. This is a useful property for fishing vessels.

4.3 Sonar

Sonar (*Sound Navigation And Ranging*) is in principle very similar to an echo sounder. The main difference is that the transducer can vary the angle of the transmitted pulse and that the topography of the sea bottom is displayed on a screen. The transducer is also more advanced compared to an echo sounder and it can sometimes be submerged in the water under the hull of the ship. For navigation purposes, sonar is often used to display the seabed ahead of the ships course, Figure **??**, in order to avoid sailing in too shallow waters and to avoid dangerous obstacles. Newer sonars also have 3D representation of the topography in order for inexperienced operators to interpret the data more easily.

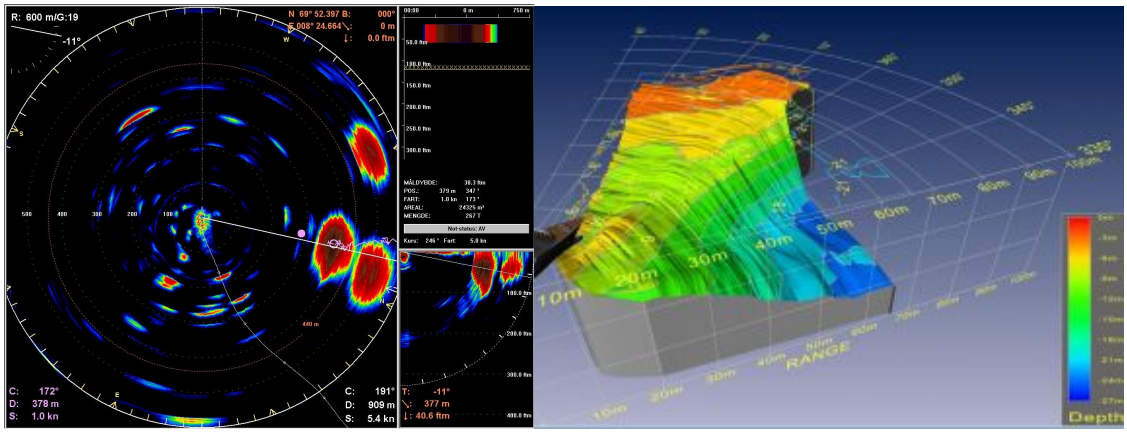

(a) 2D representation. Photo: Simrad

(b) 3D representation. Photo: Boating Business

Figure 4.2: Sonar data representations

The performance of a sonar is affected, similar to an echo sounder, by the sound speed under water. In a similar fashion, performance can be improved by measuring salinity, temperature and pressure. High frequency sonars may also be affected by absorption. This is the reason why long range sonars uses lower frequencies, because higher frequencies are more vulnerable to absorption. Acoustic shadows can also be a major source of interference.

There are mainly two types of sonars, *active sonars* and *passive sonars*. The type of sonar that is described above is an active sonar. An active sonar transmit pulses and listens to the reflected echoes from the environment. A passive sonar on the other hand does not transmit any pulse, but only listens to the environment. Passive sonars is more commonly used in military settings, where stealth requirements must be met, and also in scientific surveys for detecting fish.

4.3.1 Multibeam Sonar

Most Multibeam sonars are mainly designed for mapping of the seabed, although its uses can extend to detection and presentation of fish and seabed type. They are usually very expensive systems and they usually operate on low frequencies (80 or 180 kHz). These systems are very similar to the multibeam echo sounder and many producers develop and market these systems as the same because they share many of the same functionalities and uses.

4.4 Hydroacoustic Positioning Systems

Hydroacoustic positioning systems are the most precise and flexible underwater positioning system available to date. The concept is similar to an echo sounder, but instead of listening to the echoes reflected from the environment and seabed, transponders are utilized to reflect the signal back to the transducer. The transponder will reflect an identifiable signal that is easily distinguishable from the echos from the surroundings. These transponders can be placed on any object that an operator wish to navigate. In addition there is a different type of transponders that continuously transmits signals regardless if it receives a signal from a transducer or not. These types of transponders together with the transducer placed on the respective vessel form a hydroacoustic positioning system.

The basic principle is to calculate the distance to the transponder based on the time difference between transmitted and received ping. The angle between the transceiver(or transponder) and the transponder relative to the vertical and horizontal plane is also measured. Depending on the type of hydroacoustic positioning system the position of the transponder or the position of the vessel can be calculated using this information. A transceiver will usually consist of several transducers in an array. In most cases the transceiver will consist of three or more transducer separated by a baseline of 10 cm or less. This will allow the system to calculate the angle of the transponder relative to the different planes in the case where only one receiver is mounted on the ship and positioning of dynamic transponders in the water is desirable.

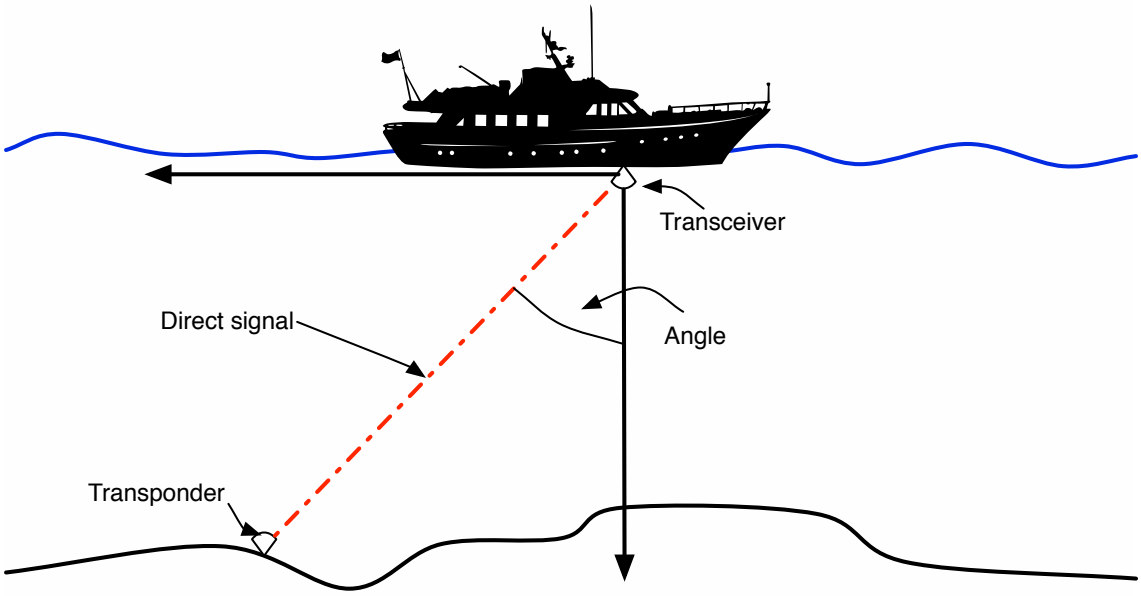

Figure 4.3: Hydroacoustic positioning principle.

There are different types of hydroacoustic positioning systems depending on the type and configuration of transponders. Some of these can be used for position of the ship whereas others are used for positioning of a transponder in the water, i.e. in the case of ROV positioning. There are mainly three categories of hydroacoustic positioning systems. These three will be explained in the following.

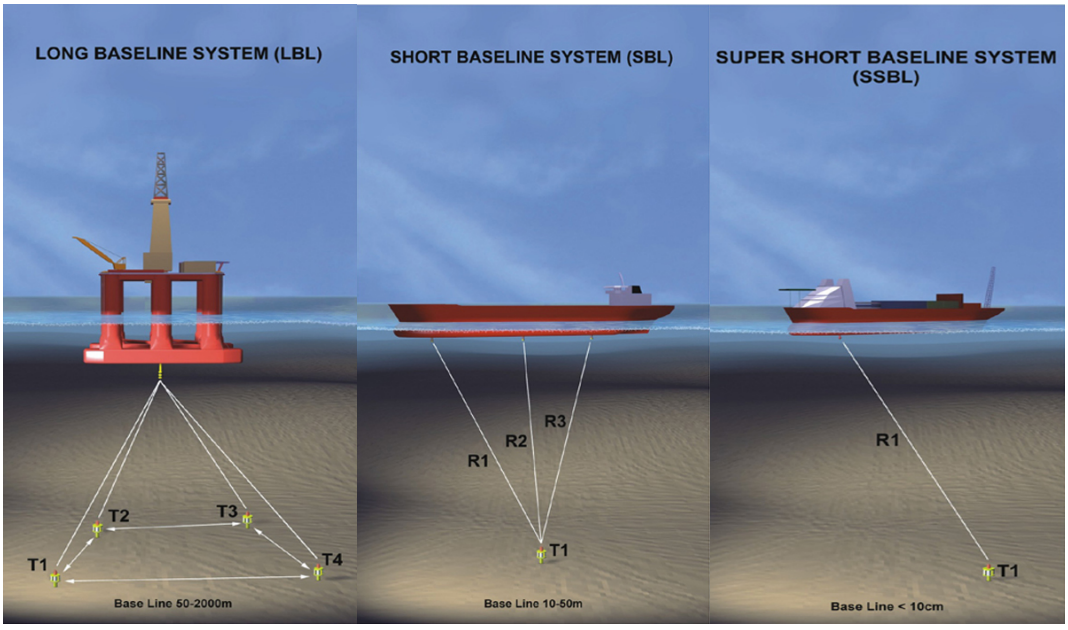

(a) LBL positioning. (b) SBL positioning. (c) SSBL positioning.

Figure 4.4: Illustration: Kongsberg Maritime.

4.4.1 Long Base Line

Long base line (LBL) positioning is based on placing a grid of transponders with fixed and known positions on the seabed. Positioning will solely rely on the distance measurement between the transducer and the different transponders on the seabed as illustrated in Figure 4.5a. This method of positioning is commonly used in deep waters, usually below 1000 meters depth. The reason for this is because the error and level of noise will increase proportionally with the distance between the transponder and the transducer. Navigation in deep waters using a transducer at sea level will therefore suffer from noise and inaccuracies. LBL is the most accurate of the hydroacoustic positioning systems with errors usually less than a foot. As seen in Figure 4.5a, the base line between the transponders on the seabed vary between 50-2000 meters.

4.4.2 Short Base Line

Short base line (SBL) positioning utilizes multiple transducers usually mounted in the aft, bow and midship positions of the hull, see Figure 4.5b. The position of the transponder is calculated using the different distances between each transducer and the transponder as well as the different angles relative to the horizontal and vertical plane. The angles are calculated based on the known baseline distances and the measured distance to the transponders. The baseline between the transceivers located on the hull of the ship will usually vary depending on the size of the ship. Usually the base line in SBL systems will be something between 10-50 meters.

4.4.3 Super Short Baseline

Super short base line (SSBL) positioning (also known as USBL, ultra short base line) uses only one transceiver to position transponders under water. In order for the system to calculate the relative angle between the horizontal and vertical frames and the transponder, the receiver consists of several transponders separated by a baseline of 10 cm or less, as explained earlier. SSBL is the simplest principle compared to LBL and SBL as it does not require extra installation of transducers on the hull or an array of transponders on the seabed. Because of the nature of how the position is calculated using the SSBL principle (and SBL for that matter), the error in the angle measurements will result in a proportional error multiplied by the distance measurement, Maritime [2011]. Accuracy can therefore be improved by measuring the angle more precisely.

4.4.4 Accuracy and Disturbances

The accuracy of these types of systems will degrade as the distance between the transponder and the transceiver or transducer increases. For LBL systems, the accuracy can usually be kept more constantly due to the redundancy in measurements. The accuracy for these types of systems will usually be $\pm$ 0.5 meters. For SBL and SSBL systems the accuracy will decrease with approximately 0.5% and 1% of the distance to the transponder respectively, Kjerstad [2010]. These numbers however, does not account for disturbances such as curvature of sound, interference, noise and sea conditions.

The performance of a hydroacoustic positioning system can be heavily affected by external conditions. Disturbances that may affect the performance are, Kjerstad [2010]:

Sea conditions. Sea conditions can create turbulence around the hull of the ship. Depending on the placement of the transceiver, this can greatly affect the performance of the positioning system.

Thruster noise. Thrusters can create noise and cavitation effect can accumulate air in the water near the transceiver. Direct vibrations from the thrusters or mechanical engines on board the vessel can also cause performance degradation of the system.

Absorption. The distance from the transceiver/transducer to the transponder can affect the performance as well due to absorption of the signal energy as described earlier.

Curvature. In conditions where the curvature of the signal is large, the performance of the system will be affected.

Water flow. Water flow might cause the transponder to deviate from the vertical plane which causes the direction of the transponder to point away from the transducer placed on the ship. Transponders that are fixed in the sea bottom will consequently not suffer from this.

Interference. Interference from other acoustic instruments can occur in areas carrying a lot of traffic. Interference can be reduced if the different vessels use their instruments on frequencies as far apart of each other as possible.

The effect of these interferences will usually all result noisier measurements and jumps in position. Spectral analysis can be performed estimate the effects to some extent in order to optimize the performance.

4.5 Doppler Velocity Log

Doppler velocity logs (DVLs) are used to measure the speed of a vessel. Calculations are based on measuring the phase shift of the reflected signal, known as the Doppler effect. The measurements are mainly based on tracking of the sea bottom (*bottom tracking*) where Doppler shifts of the signals are measured relative to the sea bed. Some DVLs also have the ability to measure the velocity of the water flow by using the same principles as above, but the doppler shifts are measured relative to scatters in the water, i.e. plankton or small particles in the water.

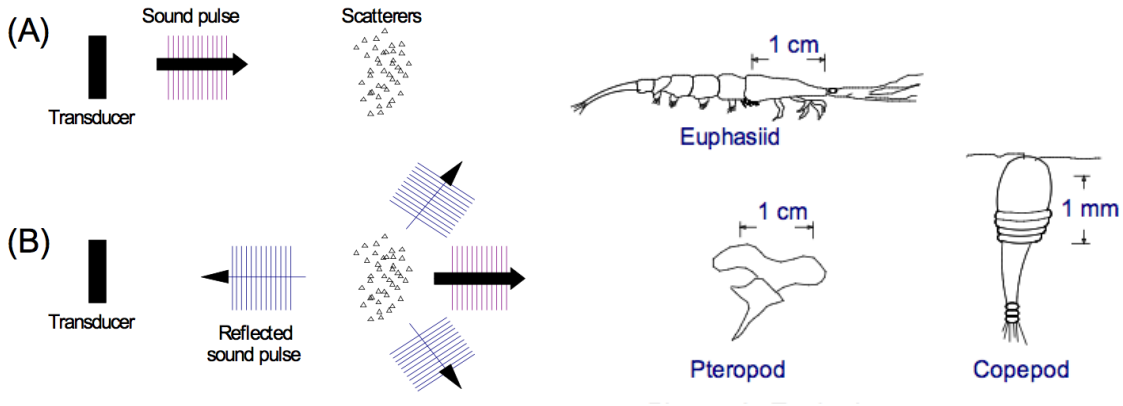

(a) Doppler shift of signal

(b) Typical ocean scatter

Figure 4.5: Illustration: RD Instruments.

The DVLs usually measure the doppler shift using separate beams. Each beam is set up such that they point in different angles. By configuring the beams to point in different directions, doppler shifts due to the heave motion of the vessel can be eliminated. DVLs are usually equipped with four beams.

4.5.1 Accuracy and Error Sources

In principle the calculated speed will have high accuracy, typically somewhere between 1-2% of the measured velocity, Kjerstad [2010]. The movement of the vessel in heave can cause disturbances. It is important to notice that the performance of the DVLs will depend on the altitude of the vessel. Because the Doppler shift of the signal is measured relative of the ocean floor, the performance is dependent on the altitude. The area of operation will also be restricted within a range of a certain altitude, depending on the type and model of DVL. The maximum operating altitude for most DVLs are around 200 meters, Instruments [2011]

Chapter 5

Inertial Navigation Systems

Inertial navigation systems (INS) are navigation systems that rely on positioning using *accelerometers* and *gyroscopes*. Inertial navigation can be defined as indicating position and velocity based on sensors that rely on the principle of Newtons laws. It is called inertial navigation because the sensors that are used measures acceleration relative to *inertial space*, which means that the measurements that are made are relative to the center of the universe. Generally, navigation is performed on a non-inertial reference frame, so the inertial sensors must account for the Earthńs rotation with respect to the inertial frame. An instrument that is used for inertial navigation is generally called an *inertial measurement unit* (IMU). There are generally two types of motion, translational and rotational. Consequently there are also two types of IMUs: the *accelerometer* and the *gyroscope*, which senses linear accelerations and rotational rate respectively, Jekeli [2001].

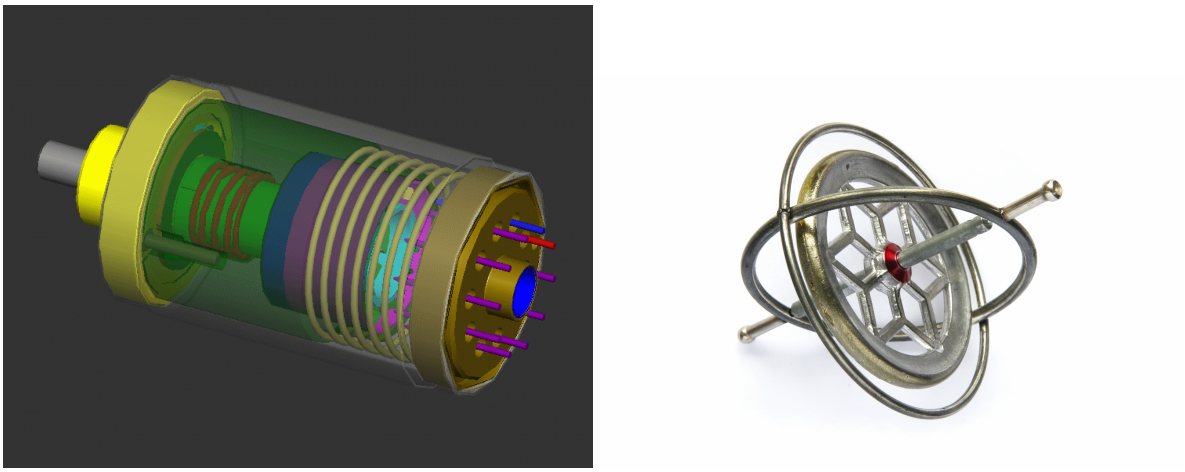

(a) A modern accelerometer.

(b) A mechanical gyroscope.

Figure 5.1: Inertial measurement units. Illustration: Sandia National Laboratories & Canadian Public Accountability Board.

5.1 Accelerometers

An accelerometer measures the linear acceleration of the device that it is mounted on. The measured acceleration is relative to the inertial frame and the accelerometer therefore measures its acceleration relative to free fall. There are many types of accelerometers that measures acceleration based on different principles. The concept behind the mechanical accelerometer will be explained as a reference. The mechanical accelerometer in one degree of freedom consists of a frame with a moving mass that is attached to a spring inside. The acceleration of the frame is thereby measured by the displacement of the spring due to the movement of the mass inside the frame as illustrated in Figure 5.2a.

If the accelerometer was in free fall, there would be no displacement of the mass inside. If the accelerometer however was placed on the ground, with the sensing axis pointing the appropriate direction, the accelerometer would measure a displacement of the mass inside. This displacement will then be equal to the Earths gravitation. A mechanical accelerometer will have certain limitations, and may also be suffering from effects such as friction and spring wear. There are many other types of accelerometers that are more precise that are based on different principles, such as the resonance based accelerometers and the laser accelerometers. Details about the principles and overview over the available types of accelerometers are referred to Jekeli [2001].

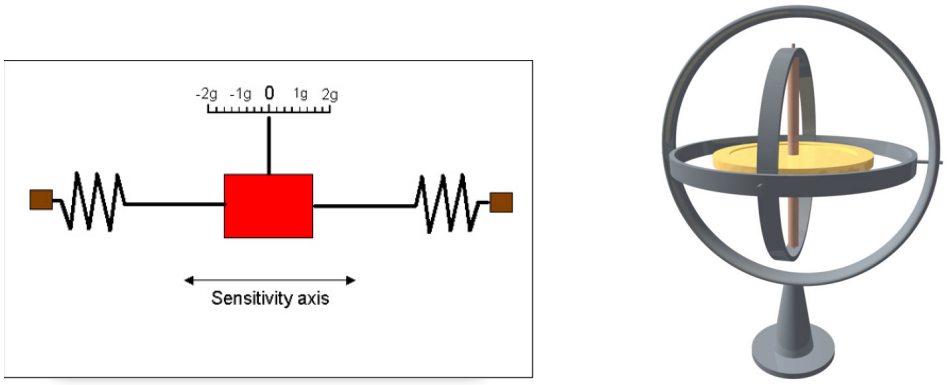

(a) A mechanical accelerometer.

(b) A mechanical gyroscope.

Figure 5.2: Mechanical accelerometer and gyroscope. Illustration: Rotoview & Creative Commons.

5.2 Gyroscopes

A gyroscope senses angular rate in relation to inertial space. The mechanical gyroscope consists of a spinning mass that is connected to a frame as illustrated in Figure 5.2b. Each of the frames that surrounds the spinning mass is perpendicular to each other. The spinning mass will have fixed rotation relative to inertial space and the orientation of the frame relative to the spinning mass is measured. Like the accelerometer, there are many types of gyroscopes that are based on different principles, like fibre optic gyroscopes and ring laser gyroscopes. Details about the concepts of these types of gyroscopes are referred to Jekeli [2001]

5.3 Performance

Because positioning using inertial navigation systems solely utilizes IMUs, the position and orientation of an object can only be found by integrating the measured states. Consequently, due to the nature of the integration process, the measurement noise will accumulate over time. This will result in a drift in position an orientation. The drift will depend on the accuracy of the sensors. The sensors therefore has be reset from time to time.

Chapter 6

Kinematics

When calculating the position of the ROV there are a few important things to consider. Many of the sensors on the vessel and on the ROV output their signals according to different reference frames. The HiPAP for example, gives the position of the ROV with respect to the tethering vessels body frame while a typical GPS gives the position with respect to an earth fixed reference frame. Also, angular movements of the vessel may cause a displacement in the position of the navigation sensors with regards to the vessels center of origin, which is usually the point where the position is calculated from. This is something that can degrade the accuracy of the calculated position if left unaddressed. Therefore, it is important to look at the conversions between the different reference frames in order to calculate the position of the ROV accurately.

6.1 Reference Frames

In navigation of marine crafts it is common to use different types of reference frames according to what type of operations that are to be performed. The needs and requirements of the navigational reference frame may be different for local navigation close to the harbor than for global transitional cargo ships. The reference frames can be divided into earth fixed reference frames and geographical reference frames.

1. ECI
   Earth Centered Inertial reference frame where the axes are fixed in space. The Earth rotates relative to this reference frame about the z-axis. Newtons laws of motion apply for this reference frame and thereby also inertial navigational systems. The ECI reference frame is an Earth fixed reference frame.

2. ECEF
   Eart Centered Earth Fixed reference frame. The axes are fixed with respect to the Earths surface. Hence, the reference frame is moving with the earths rotation and relative to the ECI reference frame about the z-axis. The x-axis intersects the sphere of the Earth at the Equator and at Greenwich which corresponds to longitude 0° and latitude 0°. However, for vessels moving at relatively low speed, the ECEF reference frame can be regarded as inertial. The ECEF referance frame is an Earth fixed reference frame.

3. NED
   North East Down reference frame. The NED reference frame is defined relative to the Earths reference ellipsoid. There are many map datums that describe the Earths reference ellipsoid, but the most commonly used is the World Geodetic System 1984 (WGS84). The reference frame is tangential to the Earths surface and is moving with the respected vessel. The axes are pointing north, east and down(pointing towards the center of the Earth with positive direction downwards). The NED reference frame is a geographical reference frame.

4. BODY
   The body reference frame is a reference frame that is fixed on the object body. This reference frame moves with the body and usually has its origin someplace on the midship along the water line for marine crafts, Fossen [2010]. The position and orientation of the body is described relative to the NED frame, while velocities and angular movements and angular velocities are described in the body reference frame.

6.2 Transformation Between BODY and NED

According to Fossen [2010], the transformation between BODY and NED is done using a rotation matrix. First, the position vectors in the different reference frames must be defined.

ECEF position	$\boldsymbol{p}^e_{b/e} = \begin{bmatrix} x \\ y \\ z \end{bmatrix}$	Longitude and latitude	$\Theta_{en} = \begin{bmatrix} l \\ \mu \end{bmatrix}$
NED position	$\boldsymbol{p}^n_{b/n} = \begin{bmatrix} N \\ E \\ D \end{bmatrix}$	Euler angles	$\Theta_{nb} = \begin{bmatrix} \phi \\ \theta \\ \psi \end{bmatrix}$
Body-fixed velocity	$\boldsymbol{v}^b_{b/n} = \begin{bmatrix} u \\ v \\ w \end{bmatrix}$	Body-fixed angular velocity	$\boldsymbol{\omega}^b_{b/n} = \begin{bmatrix} p \\ q \\ r \end{bmatrix}$

Table 6.1: Position vectors

The superscripts denotes which reference frame the vector is expressed in. The subscripts denotes the reference frame of the object with respect to another reference frame. $\{e\}$ denotes the Earth fixed reference frame ECEF, $\{n\}$ denotes the NED frame and $\{b\}$ denotes the BODY frame. $\boldsymbol{v}^b_{b/n}$ denotes the linear velocity of the body with respect to the NED frame expressed in BODY. The notations of the positions and velocities are according to the SNAME standard and are defined in Table 6.2.

Description/Degree of freedom	Linear and angular velocities	Position and Euler angles
Motions in x-direction (surge)/ 1	u	x
Motions in y-direction (sway)/ 2	v	y
Motions in z-direction (heave)/ 3	w	z
Rotation about the x-axis (roll)/ 4	p	ϕ
Rotation about the y-axis (pitch)/ 5	q	θ
Rotation about the z-axis (yaw)/ 6	r	ψ

Table 6.2: Notation of SNAME for marine crafts

Now, a vector expressed in the BODY reference frame can be transformed to the NED reference frame using a rotation matrix defined in Fossen [2010] as

$$\boldsymbol{R}_b^n(\Theta_{nb}) = \tag{6.1}$$

$$\begin{bmatrix} \cos(\psi)\cos(\theta) & -\sin(\psi)\cos(\phi)+\cos(\psi)\sin(\theta)\sin(\phi) & \sin(\psi)\sin(\phi)+\cos(\psi)\cos(\phi)\sin(\theta) \\ \sin(\psi)\cos(\theta) & \cos(\psi)\cos(\phi)+\sin(\phi)\sin(\theta)\sin(\psi) & -\cos(\psi)\cos(\phi)+\sin(\theta)\sin(\psi)\cos(\phi) \\ -\sin(\theta) & \cos(\theta)\sin(\phi) & \cos(\theta)\cos(\phi) \end{bmatrix}$$

where the subscripts denotes which reference frame the transformation is coming from and the superscript denotes which reference frame the transformation rotated to. The Rotation matrix is a function of the Euler angles Θ_{nb} between $\{n\}$ and $\{b\}$. A transformation of a vector expressed in BODY can easily be transformed to NED by multiplying the vector with the rotation matrix

$$\boldsymbol{v}_{b/n}^n = \boldsymbol{R}_b^n(\Theta_{nb})\boldsymbol{v}_{b/n}^b \tag{6.2}$$

6.3 Transformation NED and ECEF

Although it is not common, some sensors outputs data in the Cartesian ECEF frame. Because ROV operations usually are local operations, navigation is done in a local reference frame. When receiving coordinates in the ECEF frame, transformation between the ECEF and NED reference frames are necessary in order to ensure navigation of the ROV. Since the NED reference frame is defined in relation to the Earths reference ellipsoid, data from the WGS84 ellipsoid is needed in the calculations.

Parameter	Description
r_e = 6378137 m	Equatorial radius of ellipsoid
r_p = 6356752 m	Polar axis radius of ellipsoid
ω_e 7.292115$\times 10^{-5}$rad/s	Angular velocity of the Earth
μ_g =39860005$\times 10^8 m^3/s^2$	Gravitational constant on Earth
e = 0.0818	Eccentricity of ellipsoid.

Table 6.3: WGS 84 parameters

Conversion from longitude and latitude coordinates to the ECEF frame for a given hight is given in Fossen [2010] as

$$\begin{bmatrix} x \\ y \\ z \end{bmatrix} = \begin{bmatrix} (N+h)\cos(\mu)\cos(l) \\ (N+h)\cos(\mu)\sin(l) \\ (\frac{r_p^2}{r_e^2}N+h)\sin(\mu) \end{bmatrix} \tag{6.3}$$

where N is the radius of the curvature in the prime vertical of the ellipsoid defined as

$$N = \frac{r_e^2}{\sqrt{r_e^2\cos^2(\mu) + r_p^2\sin^2(\mu)}}. \tag{6.4}$$

A vector expressed in $\{e\}$ can be transformed to $\{n\}$ by using a rotation matrix in a similar fashion as in section (6.2). The rotation matrix is defined in Fossen [2010] as

$$\boldsymbol{R}_n^e(\Theta_{en}) = \begin{bmatrix} -\cos(l)\sin(\mu) & -\sin(l) & -\cos(l)\cos(\mu) \\ -\sin(l)\sin(\mu) & \cos(l) & -\sin(l)\cos(\mu) \\ \cos(\mu) & 0 & -\sin(\mu) \end{bmatrix} \tag{6.5}$$

6.4 Transformation Between Ellipsoidal Coordinates and UTM

GPS receivers often output the position of the receiver in ellipsoidal coordinates. The earth is usually modeled as an ellipsoid, and as mentioned above, the most common reference ellipsoid model of the Earth is the WGS84 model. An important thing to remember here is not only that the intended navigation is done in a local frame, but also that the local frame in this case is a Universal Transversal Mercator (UTM) map projection. One of the properties of a map projection is that it represents the Earth as a *flat* map. This makes the conversion of ellipsoid coordinates and UTM coordinates a more delicate matter, as transferring coordinates that are based on an ellipsoidal model to a flat model of the Earth is a little bit more comprehensive. The conversion from ellipsoidal coordinates to UTM coordinates is described in the following. The parameters that are needed for the conversion is given in Table 6.4.

Parameter	Description
l	Longitude of point
μ	Latitude of point
l_o	Central meridian of UTM zone
k_0	Scale of central meridian of UTM zone
a	Semimajor axis of ellipsoid
b	Semiminor axis of ellipsoid
$e = \sqrt{\frac{1-b^2}{a^2}}$	Eccentricity of ellipsoid
$e'^2 = \frac{e^2}{1-e^2}$	Eccentricity 2
$n = \frac{a-b}{a+b}$	-
$\rho = \frac{a1-e^2}{(1-e^2\sin^2(\mu))^{2/3}}$	Radius of curvature of the Earth in the meridian plane
$\nu = \frac{a}{\sqrt{1-e^2\sin^2(\mu)}}$	The radius of curvature of the Earth perpendicular to the meridian plane
$p = l - l_0$	(in radians)

Table 6.4: UTM conversion parameters

In order to transform ellipsoid coordinates into UTM coordinates, the arc length of the ellipsoid must be calculated. But since calculation of an elliptical arc involves elliptic integrals, which has no close solutions, the integrals has to represented as series. Calculation of the meridional arc of an ellipsoid is given in Dutch [2011] as

$$S = A'\mu - B'\sin(2\mu) + C'\sin(4\mu) - D'\sin(6\mu) + E'\sin(8\mu), \tag{6.6}$$

where μ is expressed in radians. Further, the remaining variables are defined as

$$
\begin{aligned}
A' &= a[1 - n + (5/4)(n^2 - n^3) + (81/64)(n^4 - n^5)...] && (6.7)\\
B' &= (3\tan(S/2))[1 - n + (7/8)(n^2 - n^3) + (55/64)(n^4 - n^5)...] && (6.8)\\
C' &= (15\tan^2(S/16))[1 - n + (3/4)(n^2 - n^3)...] && (6.9)\\
D' &= (35\tan^3(S/48))[1 - n + (11/16)(n^2 - n^3)...] && (6.10)\\
E' &= (315\tan^4(S/512))[1 - n...]. && (6.11)\\
& && (6.12)
\end{aligned}
$$

Alternatively, the meridional arc can also be written as

$$
\begin{aligned}
S &= a[(1 - e^2/4 - 3e^4/64 - 5e^6/256....)\mu && (6.13)\\
&\quad -(3e^2/8 + 3e^4/32 + 45e^6/1024...)\sin(2\mu)\\
&\quad +(15e^4/256 + 45e^6/1024 + ...)\sin(4\mu)\\
&\quad -(35e^6/3072 + ...)\sin(6\mu) + ...)].
\end{aligned}
$$

The UTM north, n, and east, e, position can now be calculated as, Dutch [2011]

$$
\begin{aligned}
n &= K_1 + K_2p^2 + K_3p^4 && (6.14)\\
e &= K_4^p + K_5p^3, && (6.15)\\
& && (6.16)
\end{aligned}
$$

where

$$
\begin{aligned}
K_1 &= Sk_0 && (6.17)\\
K_2 &= k_0\nu\sin(2\mu)/4 && (6.18)\\
K_3 &= [k_0\nu\sin(\mu)\cos^3(\mu)/24][5 - tan^2(\mu) + 9e'^2\cos^2(\mu) + 4e'^4cos^4(\mu)] && (6.19)\\
K_4 &= k_0\nu\cos(\mu) && (6.20)\\
K_5 &= [k_0\nu\cos^3(\mu)/6][1 - tan^2(\mu) + e'^2cos^2(\mu)]. && (6.21)\\
& && (6.22)
\end{aligned}
$$

6.5 Comparison of Kinematic Calculations

The output of the R/V Gunnerus GPS is given in WGS84 ellipsoidal coordinates. The navigation of the ROV is done in the UTM NED frame. The output of the GPS must therefore be converted to the UTM NED frame using the method described in the previous section. The HiPAP outputs the ROV position relative to the vessel body frame. It must be noted that the output of each sensor outputs the position of the *receiver*, and not the position of the vessel origin. The offsets of the sensors relative to the vessel center of origin (CO) must also be accounted for. The sensor offsets are expressed in the vessel body frame. The kinematic calculations of the navigation program transforms the HiPAP positions and the sensor offsets from the BODY frame to the NED frame using the method described in the previous sections. All these positions are then added and the result will be the ROV position.

Testing of the kinematics was done during operation of the ROV Minerva in the Trondheimsfjord on 12. May 2011. The test was set up such that the Navipac ROV position calculations was input to the navigation system. The navigation system then logged both the ROV position from Navipac and the ROV position calculated internally in the system. The results are shown in Figure 6.1 and 6.2, where the error between the two positions is plotted. The peaks that are shown in these plots are mainly due to the HiPAP raw data noise. Disregarding the noise, the kinematic calculations in north position is pretty accurate, with an error under approximately 10 cm. The east position however showed an error of about 40 cm.

Figure 6.1: Full scale test: North position comparison.

Figure 6.2: Full scale test: East position comparison.

During the test, both the ROV and the vessel was facing directly north. This means that if the difference in position is caused by a deviation in the offsets, this could easily be corrected because the vessel BODY frame is aligned with the NED frame. As a test, the HiPAP sensor offset was corrected with 10 cm and 40 cm in the corresponding directions. Figure 6.3 and 6.4 shows the results.

These results are however not conclusive. The errors may not have been caused by inaccurate sensor offsets. Because the detailed calculations of Navipac is unknown, it is hard to pinpoint the excact cause of the differences, as Navipac could for example correct the calculated positin with the DVL data or something similar. Further testing must be done in order to verify if the HiPAP corrections is the source of error or not.

It is also uncertain if the Navipac calculated ROV position is the "true" position of the ROV in the UTM NED frame. The differences in position in both navigation system is negligible as it is totally irrelevant if the ROV position is shifted 0.4 m east during most operations of the ROV Minerva. This could however be a concern if delicate operations are to be performed by the ROV near fixed locations in the seabed. The calculations and sensor offsets can however be calibrated if the AUR lab gains access to a transponder that is fixed in the seabed with a known position. This should be considered if the plans for setting up a hydroacoustic LBL system outside of the Trondheim Biological Station is followed in the future.

Figure 6.3: Full scale test: North position comparison after tuning.

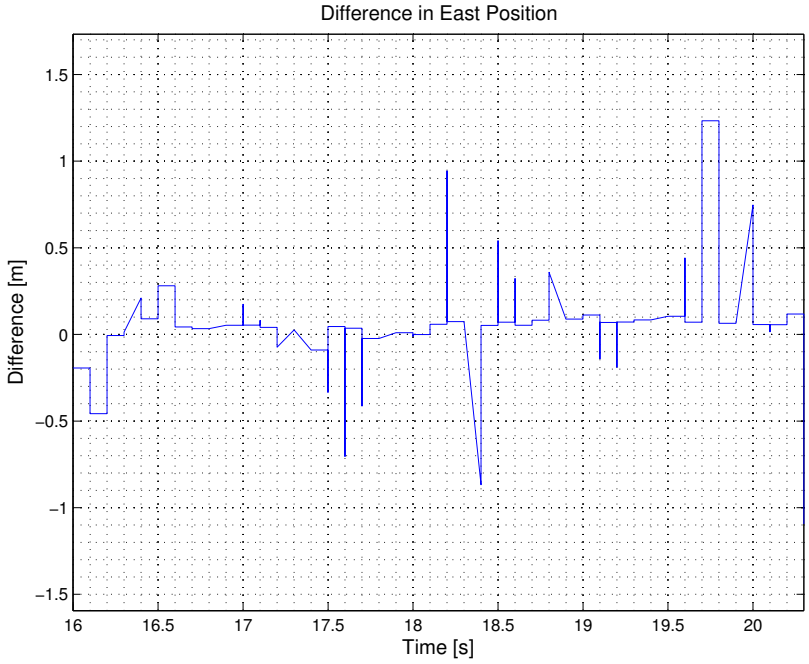

Figure 6.4: Full scale test: East position comparison after tuning.

Chapter 7

Signal processing

"Signal processing is the science of analyzing, synthesizing, sampling, encoding, transforming, decoding, enhancing, transporting, archiving and general manipulating signals in some way", Antoniou [2005].

The sensors of the vessel and ROV can be regarded as samplers and A/D converters of a real continous process.

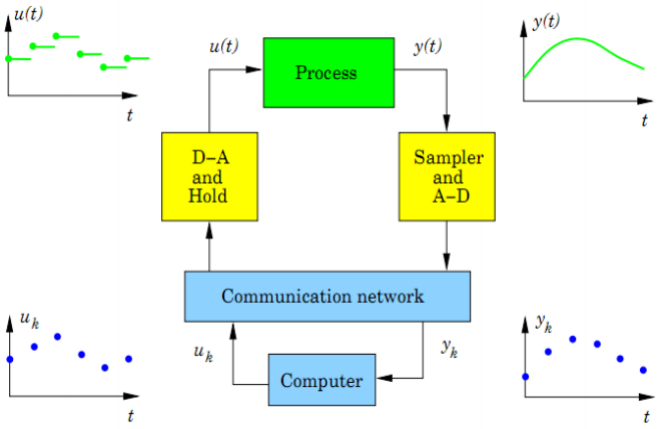

Figure 7.1: Interaction between discrete systems and continous processes

There are many aspects to consider when dealing with the integration of countinous and discrete systems. Sampling frequency, processing resources and aliasing are among the things to consider. When handling multiple sensors, the navigation system can be thought of as a single discrete system interacting with multiple continous processes. As is the case, the sensors may have different sampling periods. The HiPap for example, may have a sampling period of seconds, depending on the depth of the transponder. A GPS on the other hand may have a sampling perod of 10 hz. This is something that needs to be adressed by the navigation system and the system designer. The navigation system should output the neccessary states to the control system at a given frequency. The system should therefore be able to handle different input frequencies while giving a consistent output signal.

Signal processing in the case of a navigational system for the ROV will first and foremost consider noise filtering, signal verification, frozen or dead signals and wild point removal. The key is to acheive a robust and trustworthy system.

7.1 Noise filtering

Sensors may be subjected to noise from various sources. Noise can occur during the sampling process or due to some external disturbance. For a GPS for example, the signal to noise ratio(SNR), will vary with the frequency of the signal. At low frequencies external noise from the surroundings will dominate whereas for high frequencies, the internal noise of the GPS receiver and signal amplifier will dominate the SNR, Kjerstad [2010]. Some GPS receivers may also be affected by other electronic equipment like other antennas, voltage adapters and luminous light tubes. Different types of filters can be utilized to ensure smoother signals.

7.1.1 Wiener filter

The wiener filter is not as common as one might think. Wiener theory requires the signal as well as the noise to be noiselike in character, Brown and Hwang [1997]. This is usually not the case in usual communication problems, where the signals can be described in a somehow deterministic way and often it is not reasonable to assume that the signal is random. For instrumentation applications however, redundant sensors can be used to combine information in order to minimize instrumentation errors. This can be useful when developing a dynamic positioning system because many DP vessels have redundant sensors in order to meet certain classification rules.

A Wiener filter minimizes the mean square estimation error by a weighting function approach. The challenge is to figure out how the past history of the input should be weighted in order to acheive the best estimate of the variable of interest.

In Brown and Hwang [1997], the input is considered to be a series of noisy measurements

$$z_1, z_2, z_3, \ldots, z_n \tag{7.1}$$

where each measurement z_i is an additive combination of signal and noise, $z_1 = s_1 + n_1, z_2 = s_2 + n_2$, and so forth. The corresponding output of the filter is denoted $x_1, x_2, x_3, \ldots, x_n$. The output at a given time t_n can be expressed as a general linear combination of the past measurements

$$x_n = k_1 z_1 + k_2 z_2 + \ldots + k_n z_n. \tag{7.2}$$

Hence, the filter error can be written as

$$\begin{aligned} e_n &= s_n - x_n & (7.3)\\ &= s_n - (k_1 z_1 + k_2 z_2 + \ldots + k_n z_n). & (7.4) \end{aligned}$$

The mean square error is then written as

$$\begin{aligned} E(e_n^2) &= E[s_n - (k_1 z_1 + k_2 z_2 + \ldots + k_n z_n)]^2 \\ &= E(s_n^2) + [k_1^2 E(z_1^2) + k_2^2 E(z_2^2) + \ldots + k_n^2 E(z_n^2) \\ &\quad +2k_1 k_2 E(z1z2) + 2k_1 k_3 E(z_1 z_3) + \ldots] \\ &\quad -[2k_1 E(z1_s n) + 2k_2 E(z2_s n) + \ldots + 2k_n E(z n_s n)] \end{aligned} \tag{7.5}$$

Further, the factors $k_1, k_2, \ldots, k_n$ must be found such as to minimize $E(e_n^2)$. 7.5 can now be defined as a linear set of equations by the use of usual differential calculus, Brown and Hwang [1997].

$$\begin{bmatrix} E(z_1^2) & E(z_1 z_2) & \cdots & \cdots \\ E(z_2 z_1) & \ddots & & \\ \vdots & & \ddots & \\ E(z_n z_1) & & & E(z_n^2) \end{bmatrix} \begin{bmatrix} k_1 \\ k_2 \\ \vdots \\ k_n \end{bmatrix} = \begin{bmatrix} E(z_1 s_n) \\ E(z_2 s_n) \\ \vdots \\ E(z_n s_n) \end{bmatrix} \tag{7.6}$$

It is assumed that the auto- and crosscorrelation functions of the signal and noise are known, so that (7.6) can be solved for the factors $k_1, k_2, \ldots, k_n$. It is clear that for each measurement z_i, the problem size increases. This is something that can easily get out of hand. One way to get around this problem is to only account for the n most recent measurements and thereby disregard all measurements before z_{i-n}.

7.1.2 Kalman filter

A Kalman filter is basically a recursive solution to the discrete-data linear filtering problem. The Kalman filter was first introduced by Rudy E. Kalman in his paper in 1960. The Kalamn filter became very popular almost immediately and still is widely used today mainly because of its ease of implementation in real time applications, its extendability and effectiveness.

From Brown and Hwang [1997], the state $\boldsymbol{x}$ of the random process to be estimated can be modeled in the form

$$\boldsymbol{x}_{k+1} = \boldsymbol{\phi}_k \boldsymbol{x}_k + \boldsymbol{w}_k, \tag{7.7}$$

where $\boldsymbol{\phi}_k$ is the state transition matrix relating $\boldsymbol{x}_k$ to $\boldsymbol{x}_{k+1}$ and $\boldsymbol{w}$ is a white sequence with known covariance structure. The measurement $\boldsymbol{z}$ of the process is assumed to consist of the following linear relationship

$$\boldsymbol{z}_k = \boldsymbol{H}_k \boldsymbol{x}_k + \boldsymbol{v}_k, \tag{7.8}$$

where $\boldsymbol{H}_k$ is a matrix giving the connection between the measurement and the state and $\boldsymbol{v}_k$ is the measurement error with known covariance structure and zero crosscorrelation with the $\boldsymbol{w}_k$ sequence.

Further, the covariance matrices for the vectors $\boldsymbol{w}_k$ and $\boldsymbol{v}_k$ are given by

$$E[\boldsymbol{w}_k \boldsymbol{w}_i^T] = \begin{cases} \boldsymbol{Q}_k, & i = k \\ 0, & i \neq k \end{cases} \tag{7.9}$$

$$E[\boldsymbol{v}_k \boldsymbol{v}_i^T] = \begin{cases} \boldsymbol{R}_k, & i = k \\ 0, & i \neq k \end{cases} \tag{7.10}$$

$$E[\boldsymbol{w}_k \boldsymbol{v}_i^T] = 0, \quad \text{for all } k \text{ and } i. \tag{7.11}$$

It is assumed that an initial estimate of the process is available at time t_k. The prior estimate is denoted $\hat{\boldsymbol{x}}_k^-$. It is also assumed that the error covariance matrix associated with $\hat{\boldsymbol{x}}_k^-$ is known. The error estimation is defined to be

$$\boldsymbol{e}_k^- = \boldsymbol{x}_k - \hat{\boldsymbol{x}}_k^-. \tag{7.12}$$

The associated error covariance matrix is

$$\boldsymbol{P}_k^- = E[\boldsymbol{e}_k^- \boldsymbol{e}_k^{-T}] = E[(\boldsymbol{x}_k - \hat{\boldsymbol{x}}_k^-)(\boldsymbol{x}_k - \hat{\boldsymbol{x}}_k^-)^T]. \tag{7.13}$$

The estimation problem becomes a linear blending of the prior estimate and the noisy measurement

$$\hat{\boldsymbol{x}}_k = \hat{\boldsymbol{x}}_k^- + \boldsymbol{K}_k(\boldsymbol{z}_k - \boldsymbol{H}_k \hat{\boldsymbol{x}}_k^-) \tag{7.14}$$

where

$$\begin{aligned} \hat{\boldsymbol{x}}_k &= \text{updated estimate} \\ \boldsymbol{K}_k &= \text{Kalman gain (blending factor).} \end{aligned}$$

The problem is to find a Kalman gain $\boldsymbol{K}_k$ such that the estimate is updated is some optimal sense. As with the Wiener filter, a minimum mean square error criterion is used. First, the expression for the error covariance for the updated estimate is formed as

$$\boldsymbol{P}_k = E[\boldsymbol{e}_k \boldsymbol{e}_k^T] = E[(\boldsymbol{x}_k - \hat{\boldsymbol{x}}_k)(\boldsymbol{x}_k - \hat{\boldsymbol{x}}_k)^T]. \tag{7.15}$$

Substituting (7.8) into (7.14) results in

$$\begin{aligned} \boldsymbol{P}_k = E\{ & [(\boldsymbol{x}_k - \hat{\boldsymbol{x}}_k^-) - \boldsymbol{K}_k(\boldsymbol{H}_k \boldsymbol{x}_k + \boldsymbol{v}_k - \boldsymbol{H}_k \hat{\boldsymbol{x}}_k^-)] \\ & [(\boldsymbol{x}_k - \hat{\boldsymbol{x}}_k^-) - \boldsymbol{K}_k(\boldsymbol{H}_k \boldsymbol{x}_k + \boldsymbol{v}_k - \boldsymbol{H}_k \hat{\boldsymbol{x}}_k^-)]\}. \end{aligned} \tag{7.16}$$

This can now be rewritten as

$$\boldsymbol{P}_k = (\boldsymbol{I} - \boldsymbol{K}_k\boldsymbol{H}_k)\boldsymbol{P}_k^-(\boldsymbol{I} - \boldsymbol{K}_k\boldsymbol{H}_k) + \boldsymbol{K}_k\boldsymbol{R}_k\boldsymbol{K}_k^T. \tag{7.17}$$

The idea now is to find a $\boldsymbol{K}_k$ such that the individual terms along the major diagonal of $\boldsymbol{P}_k$ is minimized. These terms represent the error variances for the elements of the state vector being estimated. The estimation can be done in a number of ways. A straightforward approach using differential calculus will be shown.

In [Turkington, 2002, p.80], two different matrix differential formulas are given as

$$\frac{d[\text{trace}(\boldsymbol{AB})]}{d\boldsymbol{A}} = \boldsymbol{B}^T(\boldsymbol{AB} \text{ must be square}) \tag{7.18}$$

$$\frac{d[\text{trace}(\boldsymbol{ABA}^T)]}{d\boldsymbol{A}} = 2\boldsymbol{AC}(\boldsymbol{C} \text{ must be symmetric}). \tag{7.19}$$

The updated error covariance matrix can be expanded on the form

$$\boldsymbol{P}_k = \boldsymbol{P}_k^-\boldsymbol{K}_k\boldsymbol{H}_k\boldsymbol{P}_k^- - \boldsymbol{P}_k^-\boldsymbol{H}_k^T\boldsymbol{K}_k^T + \boldsymbol{K}_k(\boldsymbol{H}_k\boldsymbol{P}_k^-\boldsymbol{H}_k^T + \boldsymbol{R}_k)\boldsymbol{K}_k^T. \tag{7.20}$$

Taking the derivative of the trace of the updated error covariance matrix with respect to the Kalman gain while using (7.19) yields

$$\frac{d(\text{trace}\boldsymbol{P}_k)}{d\boldsymbol{A}} = -2(\boldsymbol{H}_k\boldsymbol{P}_k^-)^T + 2\boldsymbol{K}_k(\boldsymbol{H}_k\boldsymbol{P}_k^-\boldsymbol{H}_k^T + \boldsymbol{R}_k) \tag{7.21}$$

Setting the derivative to zero and solving for $\boldsymbol{K}_k$ yields

$$\boldsymbol{K}_k = \boldsymbol{P}_k^-\boldsymbol{H}_k^T(\boldsymbol{H}_k\boldsymbol{P}_k^-\boldsymbol{H}_k^T + \boldsymbol{R}_k)^{-1} \tag{7.22}$$

Substitution of (7.22) into (7.20) leads to

$$\boldsymbol{P}_k = (\boldsymbol{I} - \boldsymbol{K}_k\boldsymbol{H}_k)\boldsymbol{P}_k^-. \tag{7.23}$$

Note that the substitution above can yield several equivalent equations and that some of them may give different results in the case when $\boldsymbol{K}_k$ is not an optimal gain. This is further discussed in Brown and Hwang [1997]. There is now means to find an optimal estimate of the state vector $\hat{\boldsymbol{k}}_k$ based on (7.14) and (7.22). In order to calculate the estimate for the next step, the prior estimates of the state and error covariance ,$\hat{\boldsymbol{x}}_k^-$ and $\boldsymbol{P}_k^-$, must be updated. The prior state estimate is updated using the state transition matrix.

$$\hat{\boldsymbol{x}}_{k-1}^- = \boldsymbol{\phi}_k\hat{\boldsymbol{x}}_k. \tag{7.24}$$

The error covariance matrix associated with $\hat{\boldsymbol{x}}_{k+1}^-$ can be found by first combining (7.7), (7.12) and (7.24) to getting an expression for the prior error

$$\boldsymbol{e}_{k+1}^{-} = \boldsymbol{\phi}_k \boldsymbol{e}_k + \boldsymbol{w}_k. \tag{7.25}$$

Since $\boldsymbol{w}_k$ and $\boldsymbol{e}_k$ have zero crosscorrelation, (7.13) can be rewritten for the next step as

$$\boldsymbol{P}_{k+1}^{-} = E[\boldsymbol{e}_{k+1}^{-} \boldsymbol{e}_{k+1}^{-T}] = \boldsymbol{\phi}_k \boldsymbol{P}_k \boldsymbol{\phi}_k^T + \boldsymbol{Q}_k. \tag{7.26}$$

With this, the equations for the recursive Kalman filter algorithm are the equations: (7.22), (7.14), (7.23), (7.25) and (7.26). The recursive algorithm can be illustrated by a figure.

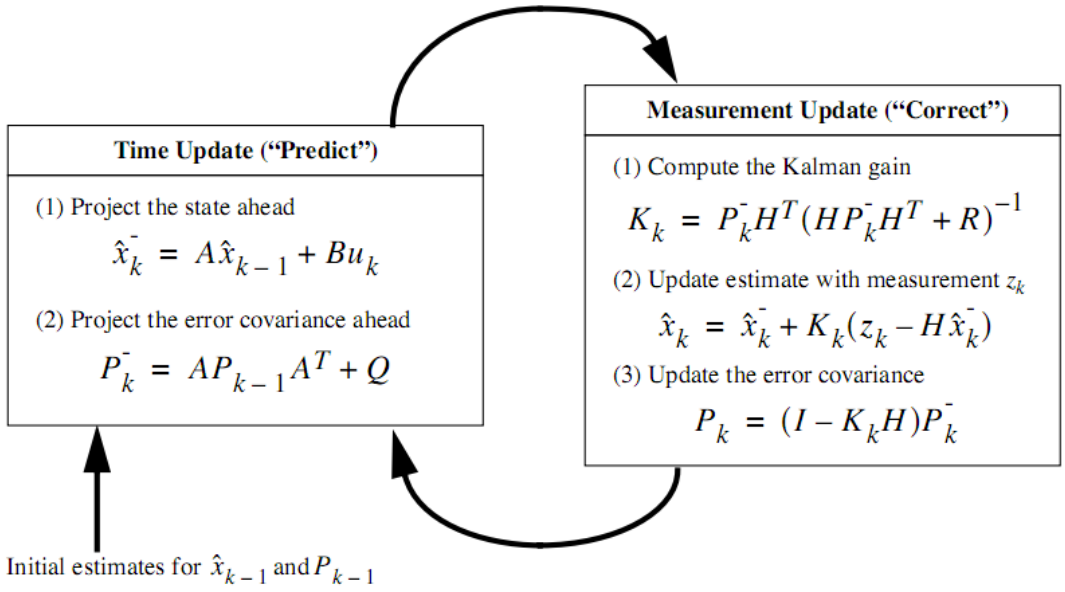

Figure 7.2: The Kalman filter recursive process. Illustration taken from Welch and Bishop [2001]

This is basic outline of the Kalman filter as presented by Rudy Kalman in 1960, Brown and Hwang [1997]. There are many extensions of the Kalman filter. The filter can be extended to incorporate prediction, nonlinearaties (the Extended Kalman filter) and observer capabilites. Details on these extensions are referred to Brown and Hwang [1997] and Fossen [2010].

7.2 The Kalman Filter of the Implemented Navigation System

A Kalman filter was implemented in the navigation system with the intention to add robustness to the system by combining independent position and velocity measurements in addition to heading and yaw rate. The current state of the Kalman filter that has been implemented suffers from some bugs. It is functional and acts as a noise filter when in operation, but there are some bugs in the filter when trying to run drop out tests. Unfortunately, attention was prioritized towards other parts of the navigation system during preparations for full scale testing. The filter remains a subject for further work.

Chapter 8

Navigation System

A navigation system has been implemented and the details of the system that has been made will be presented in the following. The main functions of this navigation system is to combine the data coming from all the different sensors and send out a customized data output containing the required navigation data to the DP control system in real time. Some of the concerns when making a navigation system from the bottom up has been to acquire the raw sensor signals. Different sensors may use different communication protocols to transfer data, and consequently support for these protocols has to be in place in order to acquire the needed signals. There are also many other issues that need consideration before further work on i.e. more sophisticated signal processing algorithms can take place. Issues like program loop iteration rate, timing principles when handling data with different update rates, interpretation of raw sensor formats, correct datum conversions and the sensor kinematics has to be taken care of in order to form a basis for the navigation system before moving on.

8.1 Hardware Platform

A Field-programmable Gate Array (FPGA) was chosen as the hardware base of the navigation system. A FPGA is a circuit that is programmable for the user. In other words, a FPGA allows the user to program the hardware according to the users intended use of the hardware. There are many manufacturers that build FPGAs with different capabilities and input/output (IO) configurations. The most important aspects to consider when choosing the hardware is the *real time performance* and the *IO configuration*. The IO of the hardware has to support all the different communication interfaces of the sensors that the system is going to include. Expansion capabilities should also be considered with regards to future upgrades or additions of sensors.

The hardware that is used as the interface for the navigation system is a *Compact RIO* (cRIO) Real Time Controller FPGA Chassis manufactured by *National Instruments*. The cRIO is based on a modular design where IO modules can be added according to the user needs. The cRIO can house up to 8 modules. National Instruments manufactures a range of modules with different IO interfaces and capabilities that can be chosen according to customer requirements, see example setup in Figure 8.1.

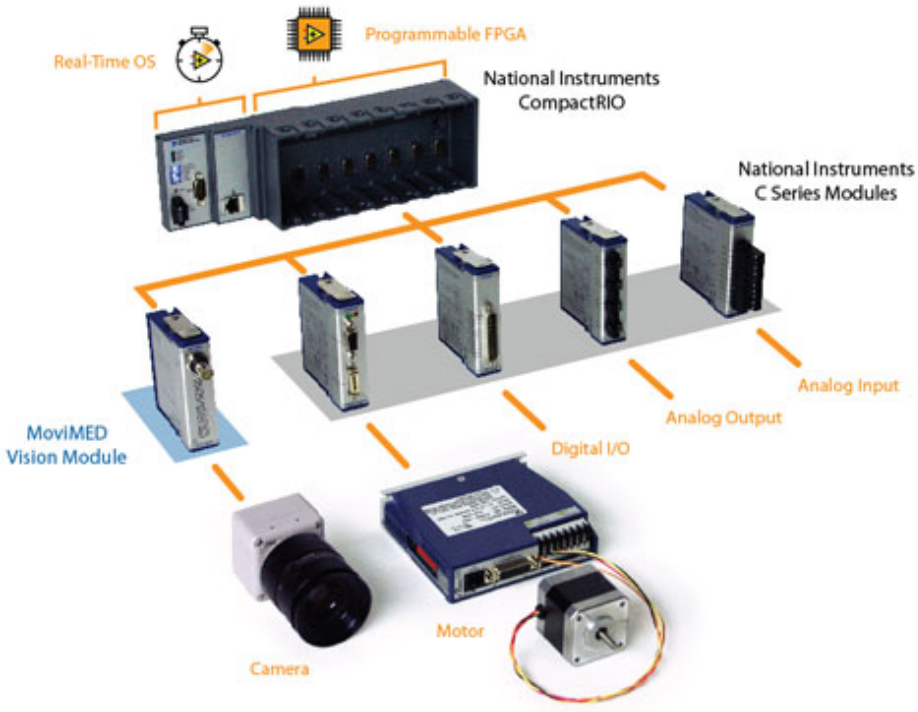

Figure 8.1: Hardware configuration example. Illustration: National Instruments

The cRIO model that is used is a cRIO 9074 together with a 9870 IO module. The technical specifications of the hardware is specified in Table 8.1.

Description	NI cRIO 9074	NI 9870 Module
Processor	400 MHz	x
Module Slots	8	x
FPGA	Spartan-3 2M	x
RAM	128 MB	x
Storage	256 MB	x
IO	2x 10/100BASE-TX Ethernet Ports + 1x RS232 Serial Port	4x RS232 Serial Ports
Power input	19-30 VDC	8-28 VDC

Table 8.1: Technical specification of hardware

8.2 Software Development Platform: National Instruments Labview

The software environment that has been used to develop the navigation system is National Instruments Labview. Labview is a graphical programming environment that is used widely by engineers and scientists to design control, measurement and test systems. The main benefits of the solutions provided by National Instruments is the tight integration between hardware and software and the broad support and developer community. Labview also has an extensive built in library of functions that can be used.

8.3 System Configuration

The navigations system will have to integrate with the already predefined IO configuration of the ROV Minerva and R/V Gunnerus sensors as well as the control system. An overview of the different interfaces that the navigation system has to interact with is shown in Figure 8.2.

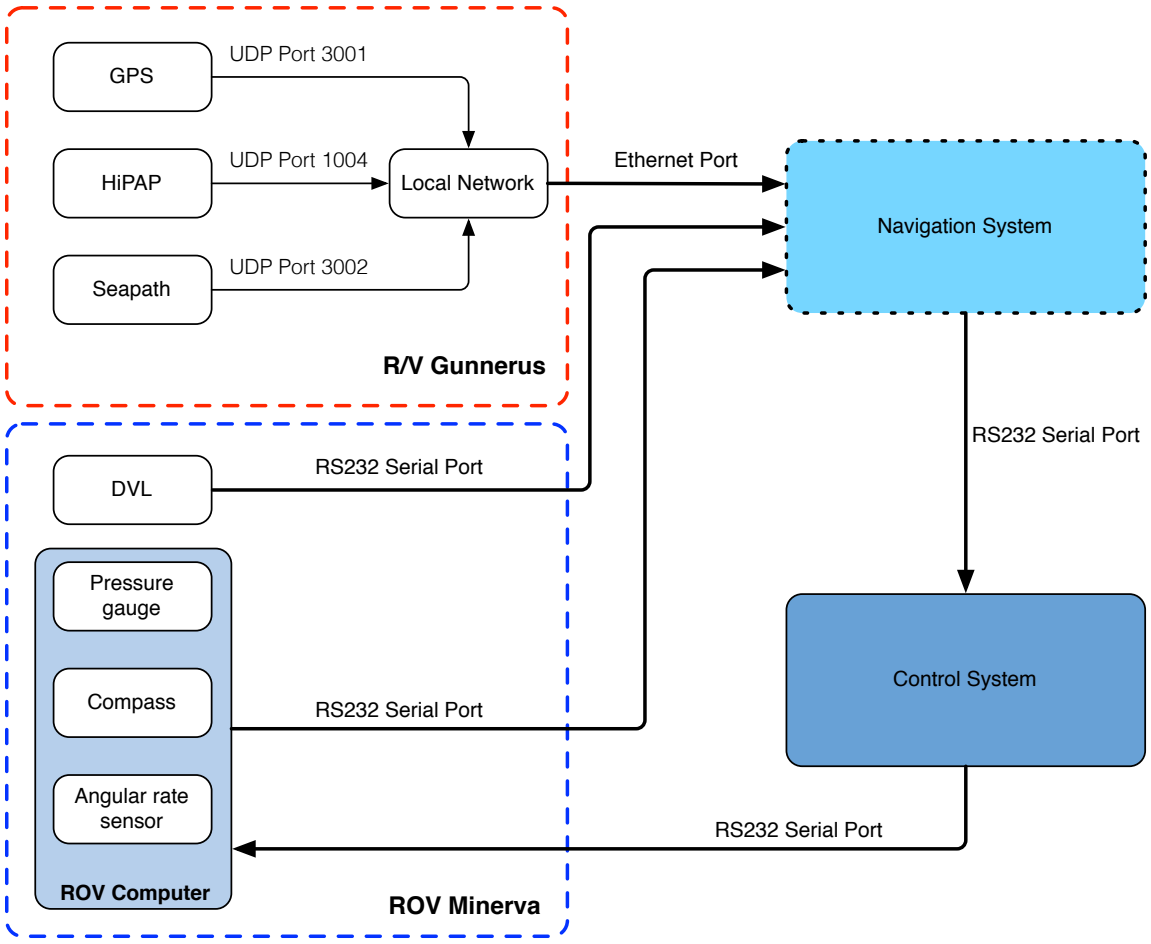

Figure 8.2: Input-output interface configuration of the R/V Gunnerus, ROV Minerva and control system.

The GPS, HiPAP and Seapath sensors broadcast their raw data on the local network on board the R/V Gunnerus using User Data Protocols (UDP) [1]. The sensors on the ROV, except for the DVL, is accessible through the ROV computer which feeds the signals straight through without any kind of processing. The ROV computer also handles the signals from other instruments on the ROV, such as the cameras. The DVL and ROV computer output data using RS232 Serial Ports. The signals from the

[1] Only the GPS and Seapath will broadcast their raw data to all IP addresses on the local network. The HiPAP will on the other hand broadcast raw data to pre-specified IP addresses. Specifying these addresses can be done from the bridge of R/V Gunnerus on the DP computer.

sensors on R/V Gunnerus can be accessed by simply connecting to the local network using a CAT5 Ethernet Cable and listening to the given UDP ports. The communication between the navigation system and the control system, which is implemented on the exact same hardware as the navigation system, is also done using a RS232 Serial Port. The control system outputs a commanded RPM thrust through a RS232 Serial Port

8.4 The Navigation Program

A navigation program has been made from the bottom up. Most of the code has been written in relation to the development of this system, but some of the functions has been borrowed and modified accordingly from the National Instruments developer community and from the control system program. The navigation program has primarily the following functions implemented:

- Read and write functions on the serial and UDP ports.
- Interpretation of sensor navigation sentences and raw formats.
- Calculation of ROV position in UTM NED coordinates based on raw sensor outputs.
- A Kalman filter combining the position, velocity, heading and yaw rate of the ROV states in the body frame.
- Logging utility, that will log all the incoming data on the different ports in separate files as well as the interpreted data inputs, outputs and relevant internal states in a master log file.
- A user interface with various controls and position plots.

A detailed description and illustration of the signal flow will be presented in Section 8.4.2.

8.4.1 Output Requirements

The ROV is currently being controlled in 4 degrees of freedom (DOF). The states that are controlled are the north [n], east [e], depth [d] and heading [ψ] positions. The output requirements of the navigation system is listed in Table 8.2.

State	Symbol	Unit	Reference Frame
North position	n	meters	NED Frame (UTM projection)
East position	e	meters	NED Frame (UTM projection)
Depth	d	meters	NED Frame (UTM projection)
Altitude	a	meters	NED Frame (UTM projection)
Surge speed	u	meters/second	Body Frame
Sway speed	v	meters/second	Body Frame
Heading	ψ	degrees	Body Frame
Yaw Rate	$\dot{\psi}$	degrees/second	Body Frame

Table 8.2: Output requirements of the navigation system

8.4.2 Signal Flow and Program Description

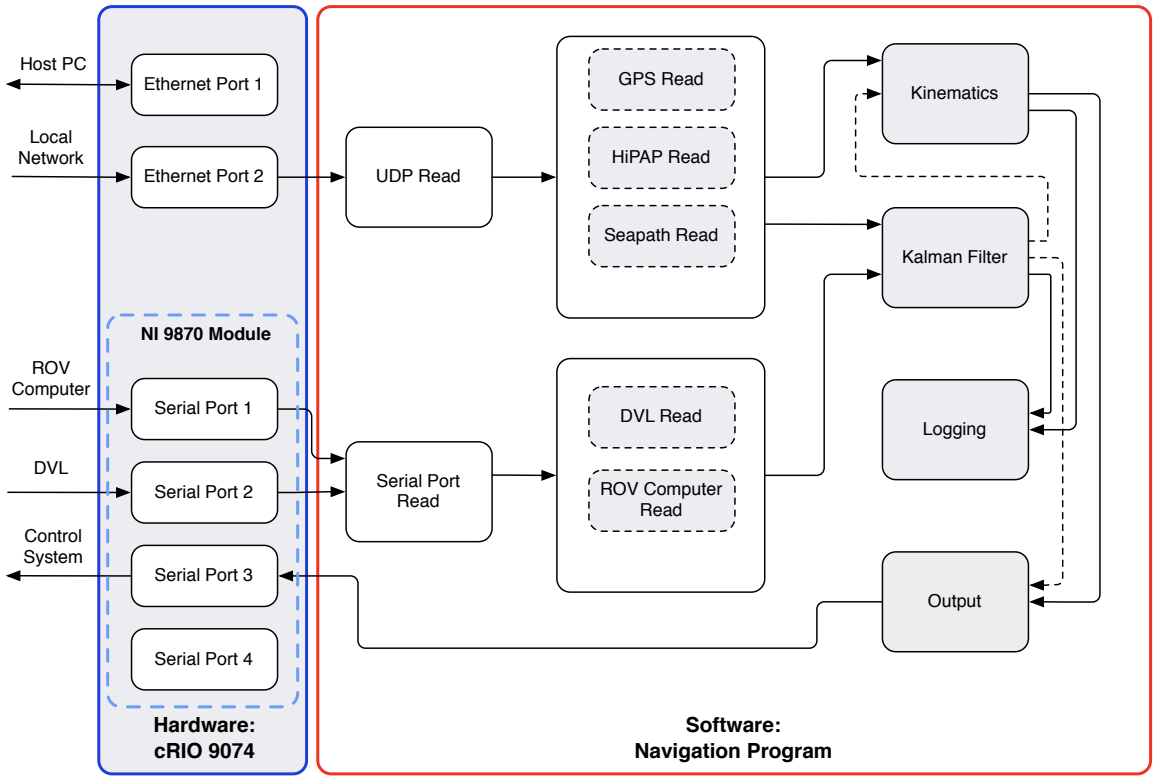

Figure 8.3: Overview of navigation program functions.

An overview of the navigation navigation program functions is shown in Figure 8.3. The sensor data is read by two functions, the *UDP Read* and the *Serial Port Read* blocks, which reads the raw navigation sentences from the sensors. Further, the navigation sentences has to be interpreted and the relevant states sorted out. After all the states has been read, the *Kinematics* block calculates the position of the ROV. Simultaneously, the raw states from the HiPAP, DVL, ROV compass and ROV angle rate is put through the *Kalman filter* block. All the raw signals, the calculated ROV position and the Kalman filter estimates is then logged by the system in the *Logging* block. An output sentence containing the data that is going to be passed to the control system is then made and written to the serial port in the *Output* block.

The program can operate in different modes. The main idea about the implementation of this navigation system is that it should be a standalone program that will also serve different purposes in the absence of the control system. It is therefore natural that the system will incorporate functions that will overlap with the control system. The use of the program without the control system, for whatever purpose, may require signal processing, such as noise filtering and state estimation. When used with the control system however, these functions may need to be bypassed as signal processing and state estimation is already implemented in the control system observer and signal processing algorithms. Filtering the raw data twice may not be desirable when evaluating the control system performance.

The system can operate in the following modes:

Bypass Mode: The Kalman filter active, but the output of the filter is bypassed and the ROV positions in the UTM NED frame is calculated using the raw data from the HiPAP, GPS and the Seapath. This is illustrated by the use of dotted lines in Figure 8.3. This is the mode that is used when operating with the control system, as filtering of the signal twice is unwanted. The estimated states are however still logged.

Kalman Filter Mode: The Kalman filter is active and the estimated states are used in the kinematic calculations and forwarded to the output.

Testing Mode: This is not intended as a mode used for operation, but rather a mode used for testing during implementation. In this mode, either the input or the output of the system can be controlled by the user in order to test performance or do debugging of implemented code.

Read & Write Functions

The read and write functions of the program consists of two functions. One function to read and write to the ethernet port and one function to read and write from the serial ports. The read and write functions for the ethernet port is pretty straight forward as Labview has built in support for communication using UDP protocols. The read and write function of the serial ports is a more comprehensive matter. Although serial communication is supported in Labview, the implementation is less intuitive. In short, the low level part of the function continuously read data from the serial ports. Each byte that is read is put into a *FIFO* (first in first out) stack. For every iteration in the main loop, the upper level of the read function reads each byte from the FIFO stack. The function utilizes just one FIFO stack for all four serial ports on the NI 9870 Module. Each byte is therefore tagged with the port number from which it is read. The upper level of the read function identifies and build the message from each port at the beginning of each iteration of the navigation system.

A problem that may occur when reading from the serial ports in this manner is that the messages from each port may be incomplete if the FIFO stack is read by the upper level function before the lower level of the function has managed to write the whole message to the stack. An algorithm to remedy this has therefore been added (courtesy of Fredrik Dukan).

Interpretation of Sensor Raw Data

The raw sensor data needs to be interpreted in order to extract the information of interest. All the sensors, except for the DVL, output their data according the the NMEA (National Marine Electronics Association) standards. Reading and extracting data from these sensors is straight forward. The DVL however, outputs its data in a proprietary binary hexadecimal format. A more comprehensive algorithm has therefore been made in order to interpret the DVL signal. The details of the format is specified in Instruments [2006]. Further details about the program code are referred to the program itself that is contained in the accompanying CD [1].

[1] To view the program code, Labview must be installed on the computer. In order to run the program, a hardware setup as described in this chapter is required because the program is written to be compiled and run on a cRIO 9074.

8.4.3 Timing Principles

The control system has a fixed loop iteration frequency of 5 Hz. This means that the navigation system has to run at 5 Hz minimum in order to feed the control system information at every iteration. The challenge is to handle all the different update rates for the different sensors simultaneously as keeping a constant output rate. The different update rates of the sensors are listed in Table 2.2.

As seen in Table 2.2, the HiPAP is the sensor with the slowest update rate and depending on the depth of the ROV, the HiPAP can use as much as a couple of seconds between each position fix. At the mean time, the navigation system has to output the ROV position at a fixed time interval. The timing principle of the navigation system is to use the *previous* data in the case where a signal is not available. This principle has been applied to all the sensors using shift registers. In other words, *zero order hold* is applied to every signal between updates.

This solution should be fine if the update rates of the sensors are faster than, or somewhere close to the navigation system iteration frequency. Should the update rate be significantly slower than the loop iteration time, the performance of the control system may suffer due to the "frozen" signal. An example can be in the case where the control system outputs a thrust force command, but is fed a constant signal in a given period of time. This may in the worst case lead to saturation of the thrusters because the control system will think that the ROV is stuck, when it actually is not. To remedy this, a Kalman filter could be used to estimate the states between the updates, but as explained earlier, it is not desirable to filter the signals twice, as the control system already has a Kalman filter observer implemented.

To solve this issue, the navigation system outputs a *flagging vector* along with the ROV states. The vector contains the status of the states in the form of 8 digits of either 1 or 0 in value. A state can then be flagged as invalid by setting the corresponding digit to the value 1. This means that if a sensor signal is not available at a given iteration, the corresponding state will be flagged invalid and the control system will recognize this and use the observer to estimate this state.

8.4.4 User Interface

A graphical user interface (GUI) has also been made for the navigation system. The user interface allow the user to control: various offsets and parameters, operating mode of the system, logging and serial port configurations among other things. The user interface also displays a position plot of the vessel and ROV relative to each other. In addition several other plots of estimation states and kinematic comparisons are also displayed [1]. Some screenshots of the GUI is provided as a reference in Figure 8.4, 8.5, 8.6 and 8.7.

[1] Kinematic comparison plots are only active when the data from the Navipac computer is input to the navigation system. This functionality was mainly implemented for testing and verification purposes.

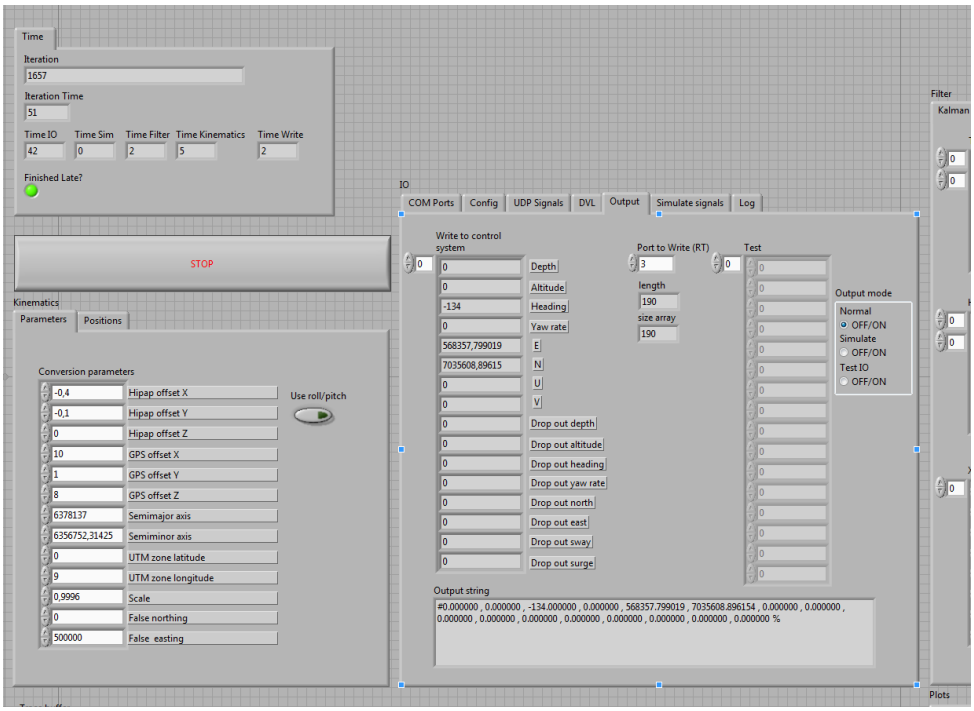

Figure 8.4: GUI: Available user controls.

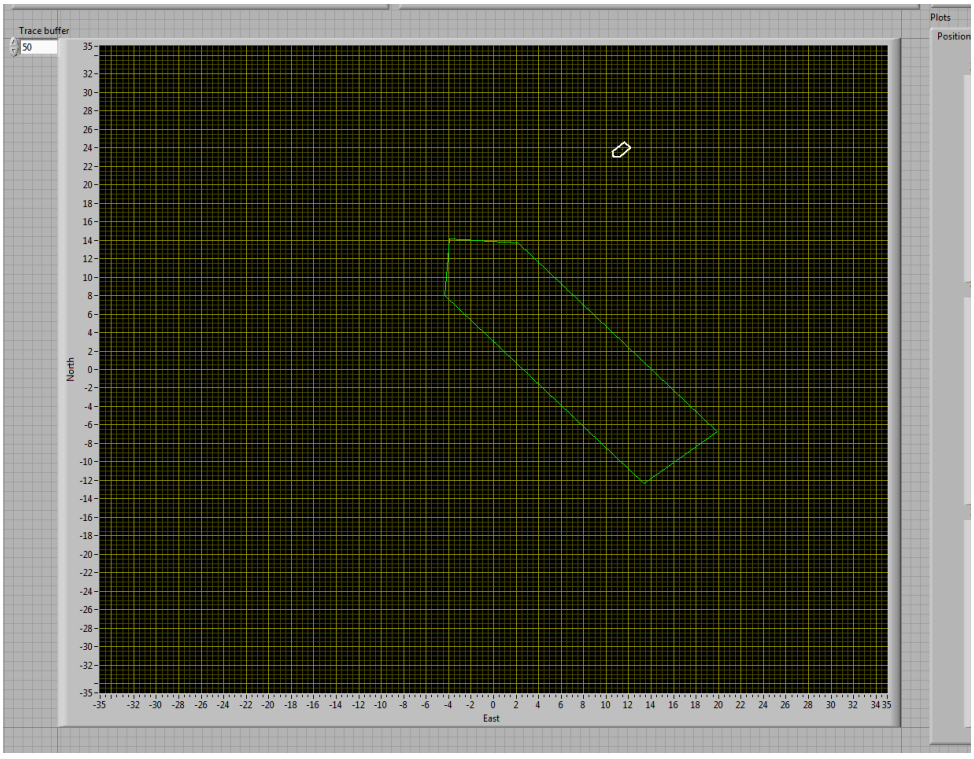

Figure 8.5: GUI: Plot of vessel and ROV position.

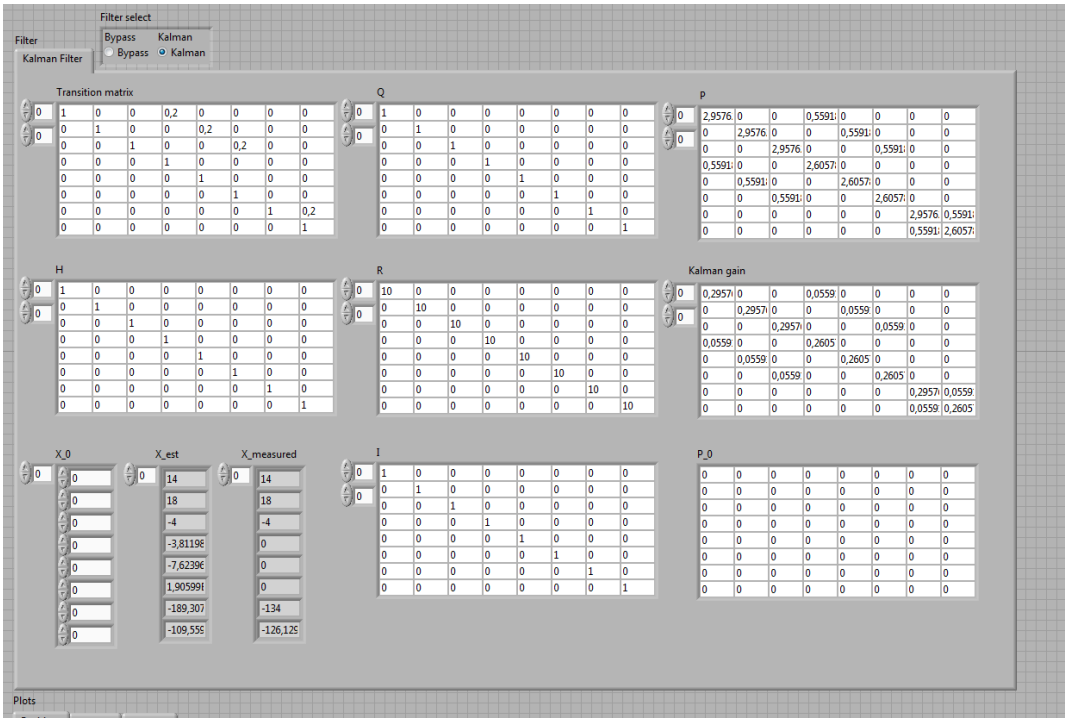

Figure 8.6: GUI: Kalman filter tuning controls.

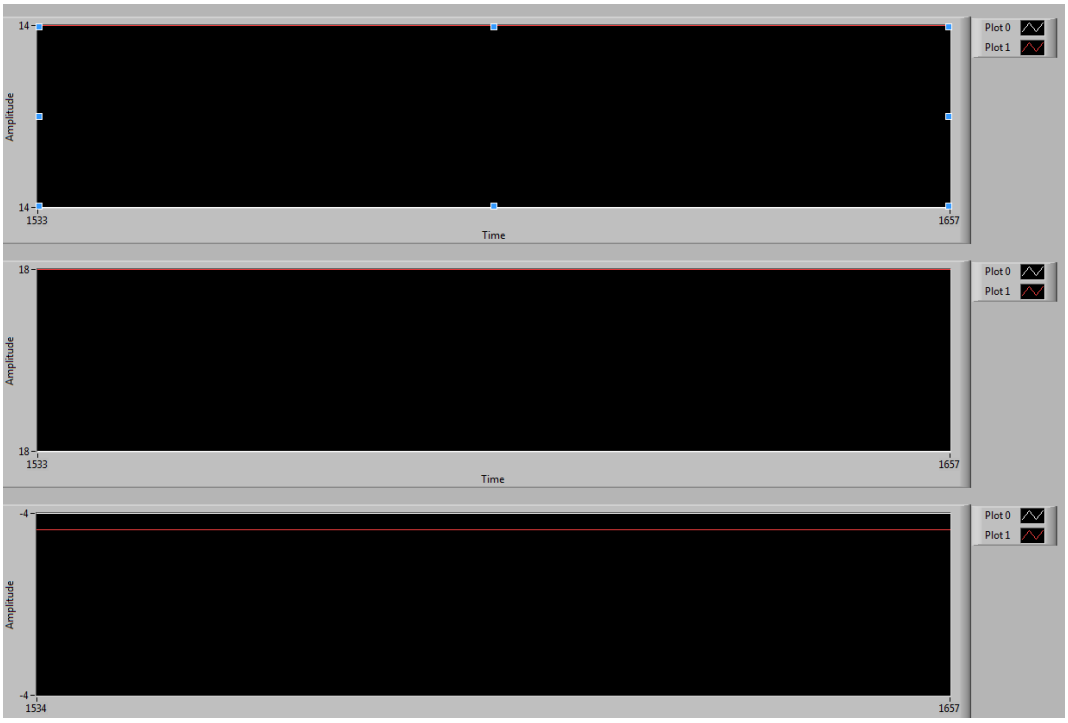

Figure 8.7: GUI: Estimated and measured states comparison.

8.4.5 Communication Between Navigation System and Control System

In the preliminary phases of the development of the navigation program, the communication between the navigation system and the control system was tested. Testing showed that there was some kind of delay between the signal that was sent from the navigation system to the control system. To investigate the matter further, a test configuration was set up. The test configuration consisted of a single source, sending a signal to both the navigation system and the control system simultaneously. Thereafter, the navigation system passed the signal unprocessed to the control system. The control system logged the signal from both the source and the navigation system and both signals were compared afterwards. Initial testing showed that the communication between the navigation system and the control system suffered from a signal delay in the magnitude of up to 5 seconds!

Debugging revealed that both the FIFO stack in the read function of the control system and the write function of the navigation system was overflowed. To remedy this, the bit rate of the serial communication between the systems was increased to 57.5 kbit/s. Any bit rate lower than this resulted in a stack overflow. Still, the communication between the two systems suffered a delay in the magnitude between of either 0.4 or 0.6 seconds (never below, above or in between!). This can be seen in Figure 8.8 and 8.9. The plotted data is the actual raw data of the yaw rate during full scale testing of the ROV in the Trondheimsfjord May 31. 2011 where a test scenario was set up as described above.

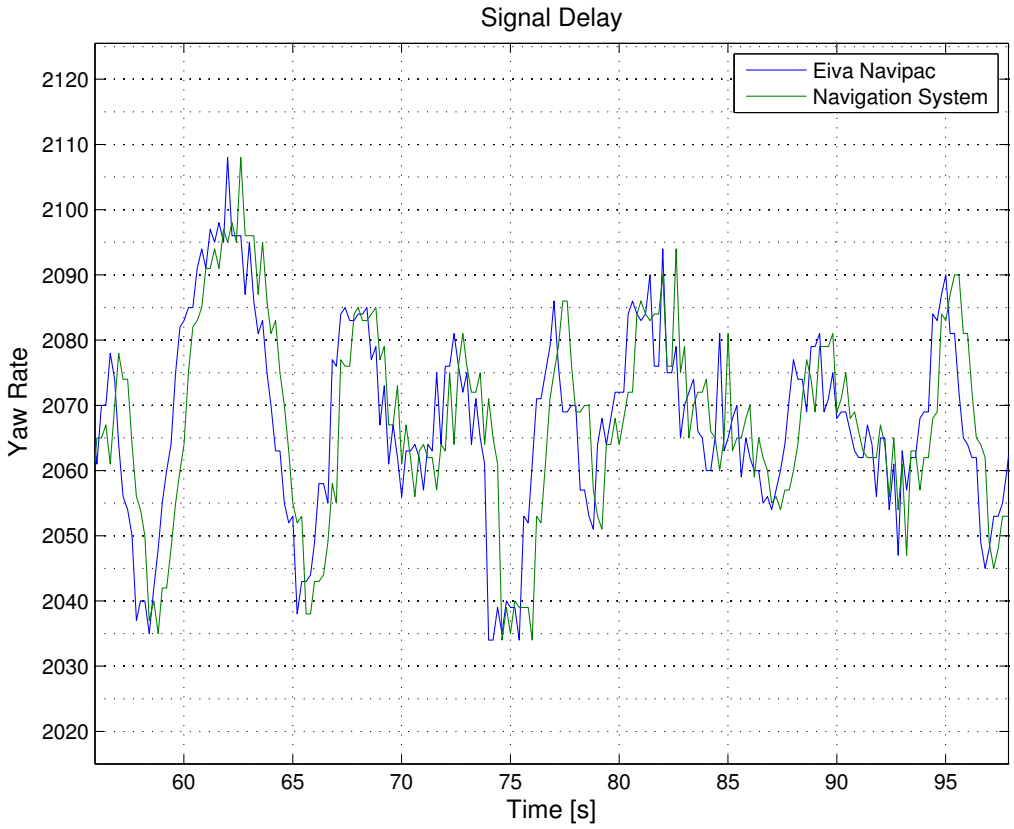

Figure 8.8: Delay between direct signal and processed signal from the navigation system.

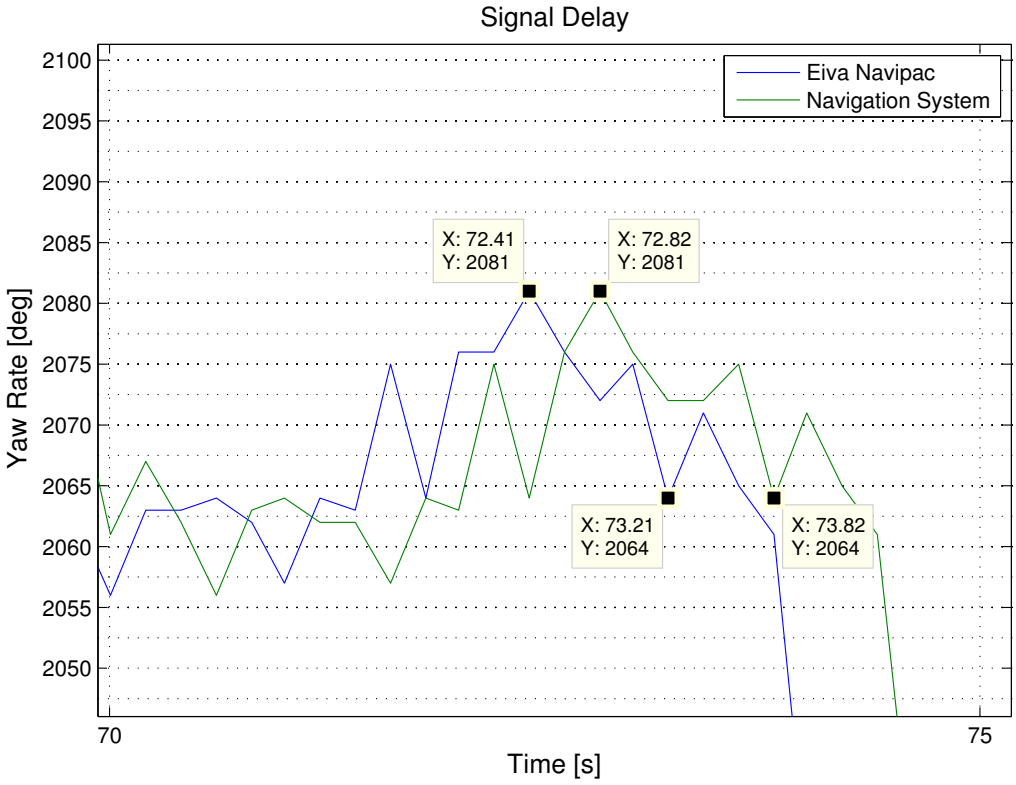

Figure 8.9: Variation and magnitude of signal delay

The size of the message that is being sent from the navigation system to the control system varies, but the message never exceeds 250 bytes. The navigation system loop iteration is run at 10 Hz, while the control system is run at 5 Hz. The read algorithm of the control system is written such that it always chooses to use the latest message that is received in the case where it receives more than one message between each iteration. Because the navigation system is run at 10 Hz, the bit rate requirements of the serial port can be calculated as

$$r = \frac{D}{\Delta T}, \tag{8.1}$$

where r is the bit rate in bits/s, D is the amount of data in bits and T is the loop iteration time in second. With $D = 250{*}8 = 2000$ and $T = 0.1$, the required bit rate can be calculated to be $r = 20000$ [bits/s]. The selected serial port bit rate should therefore be more than sufficient on both sides. In addition, monitoring of the FIFO stacks on each systems in real time shows no signs of overflow or remaining data after each iteration. In theory, the maximum delay of the signal should never exceed one loop iteration of the control system (200 ms). A signal delay of strictly either 400 ms or 600 ms strongly suggests that the bug must be connected to the loop iteration time of the control system. Most probably the bug lies within a shift register of some sort that is holding the signal between two or three loop iterations. Extensive debugging has yet managed to identify the bug. This matter should be prioritized in the further development of the navigation system.

Chapter 9

Full Scale Results and Discussion

On May 31. 2011, full scale tests were carried out with the R/V Gunnerus and the ROV Minerva in the Trondheimsfjord. The purpose was to test the performance of the navigation system in operation with the control system. The tests were successful and it may be noted that this was the first time the ROV Minerva was operated with a fully standalone system developed solely by the AUR lab! The performance of the control system when using the navigation system was tested by running two different operations with the control system. The first test shows the performance of the control system when holding a fixed position. The second test shows the performance of the control system when moving between way points. The results will be presented in the following. For comparison, operations using the navigation system Navipac made by EIVA will also be presented.

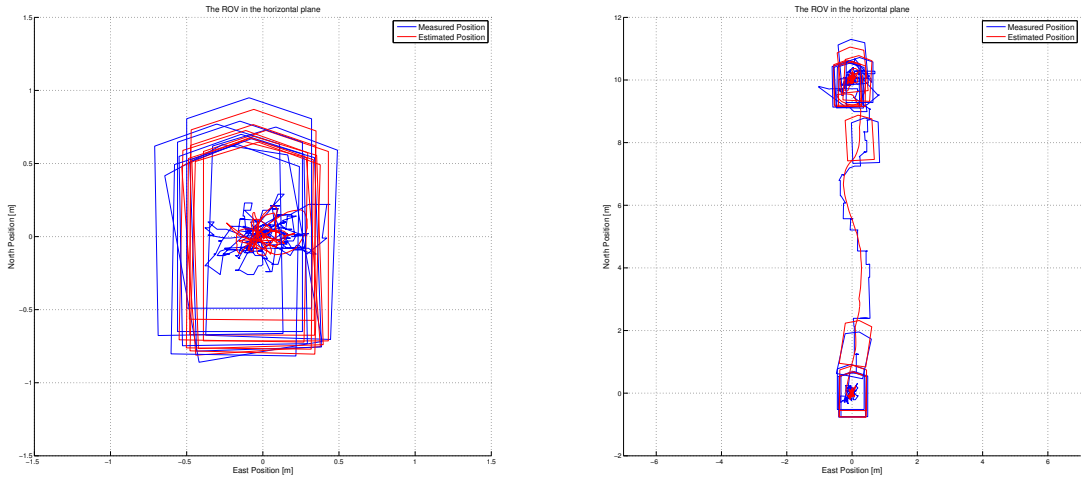

(a) Full scale test: Dynamic positioning. ROV position.

(b) Full scale test: Moving between way points. ROV position..

Figure 9.1: Full scale test scenarios.

9.1 Dynamic Positioning

The first test is a dynamic positioning test of the ROV performing station keeping. The results shows plots of the ROV position, depth, velocity, heading, yaw rate and commanded thrust. During the tests, the control system was set up such that it was able to toggle between using navigational data from the implemented navigation system and the third party Navipac system. All the tests that were performed using the implemented navigation system was done in the *Bypass Mode*.

9.1.1 Operation Using the Navigation System

As seen in Figure 9.2 and 9.3, the control system is able to hold the position of the ROV fixed with an approximate deviation of about ± 0.3 meters in north position and ± 0.4 meters in east position. The depth is pretty much kept constant at ± 10 cm as shown in Figure 9.4. The heading as shown in Figure 9.5 is a bit more varying, with a deviation of about $\pm 10°$. These results show that the system is functioning and the control system is able to operate in a dynamic positioning mode when using the implemented navigation system.

It must be noted that during approximately the first ten seconds of these plots, Navipac data was used for navigation before switching to the navigation system data. The performance of the control system using the implemented navigation system compared to Navipac will be discussed later.

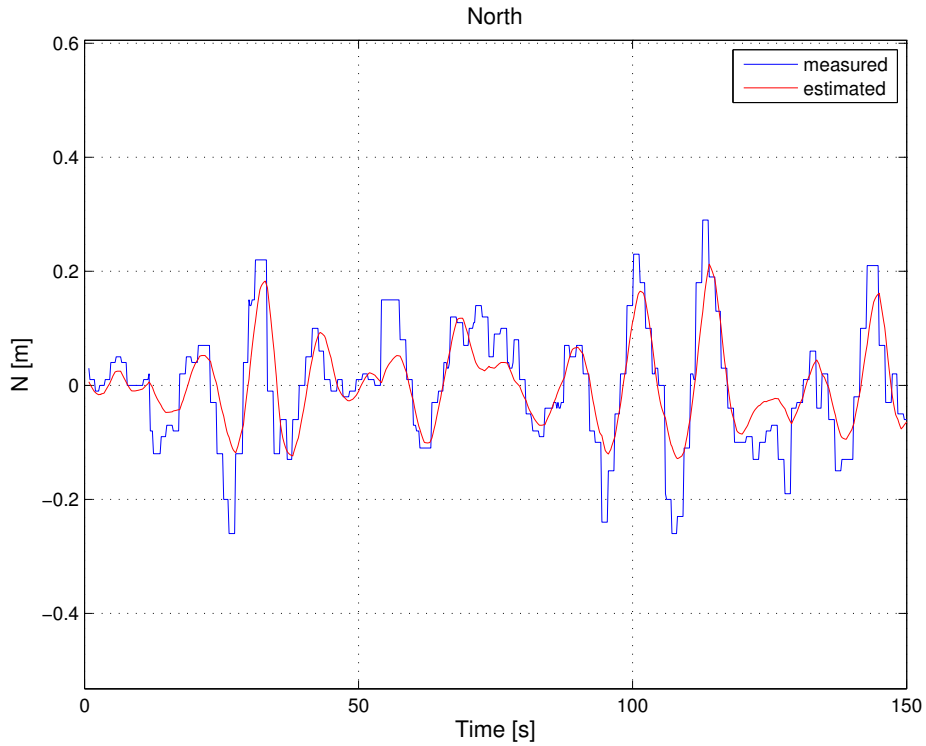

Figure 9.2: Full scale test: Dynamic positioning. North position.

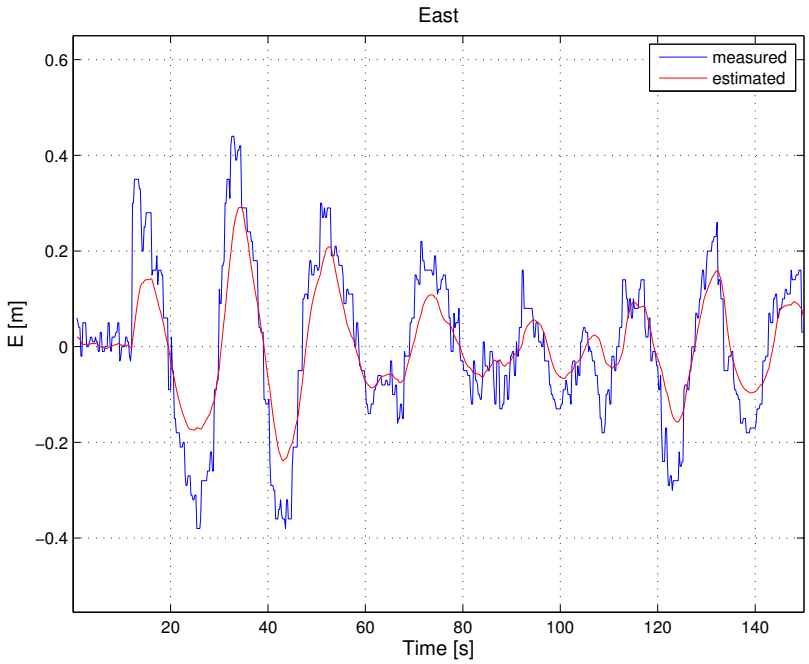

Figure 9.3: Full scale test: Dynamic positioning. East position.

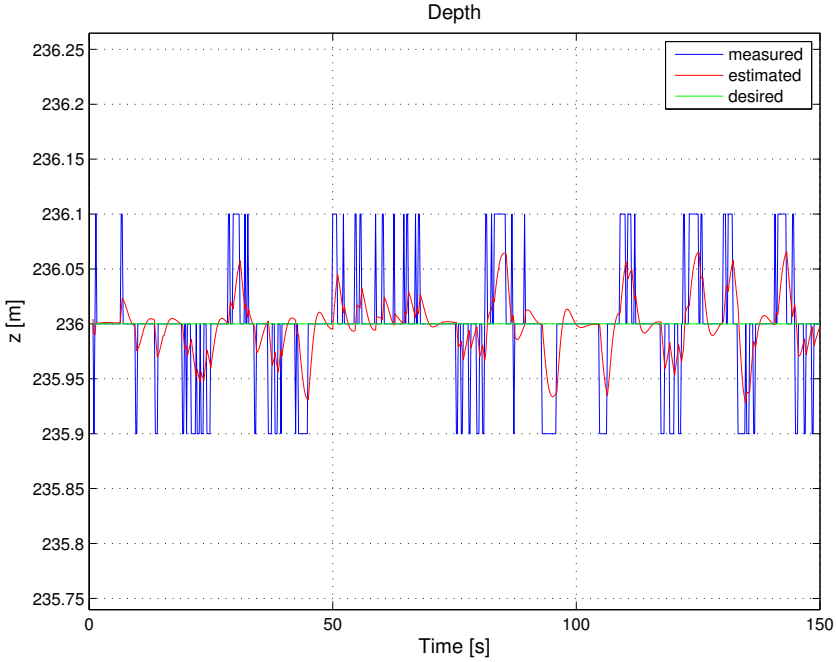

Figure 9.4: Full scale test: Dynamic positioning. Depth.

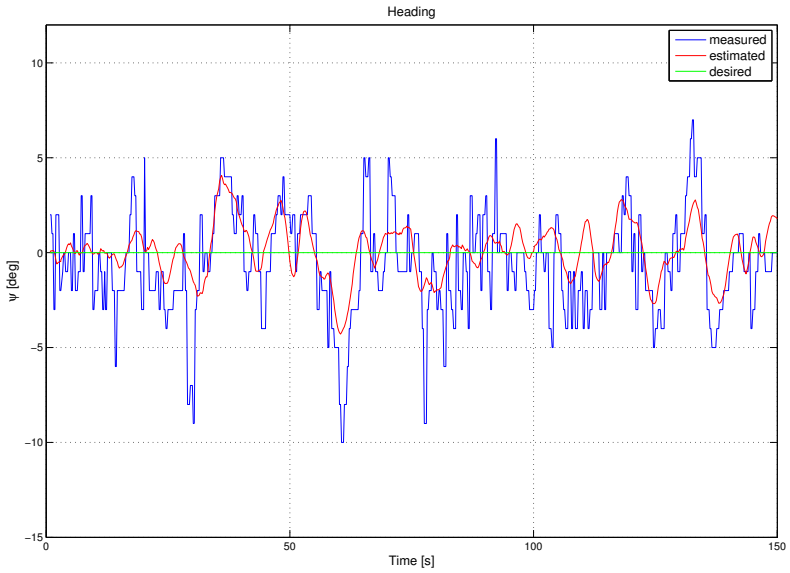

Figure 9.5: Full scale test: Dynamic positioning. Heading.

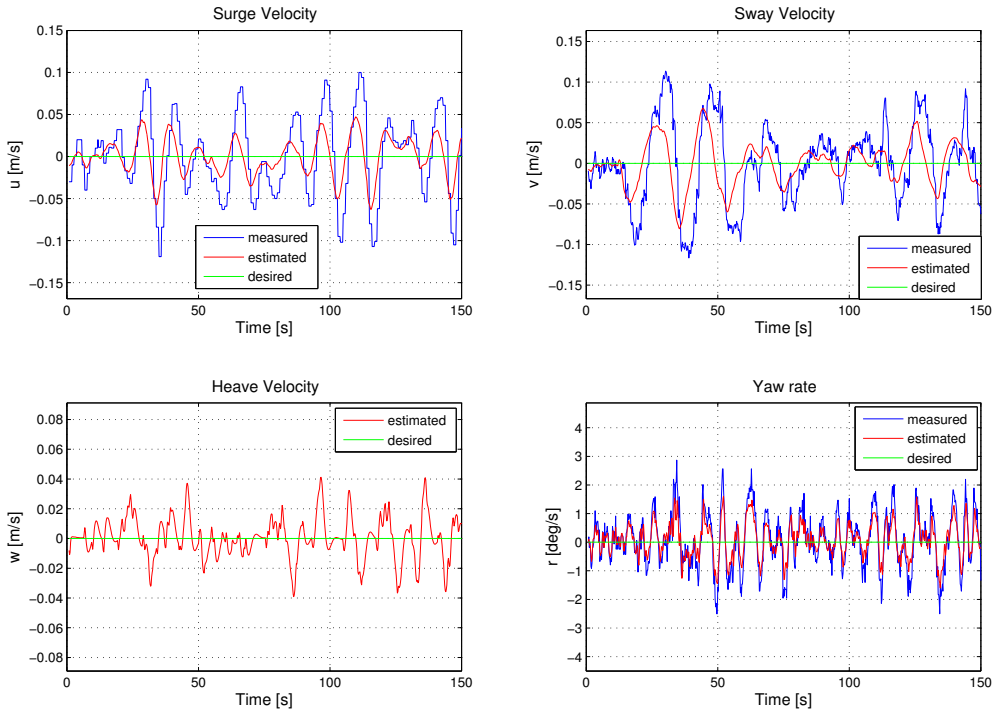

Figure 9.6: Full scale test: Dynamic positioning. Velocities and yaw rate.

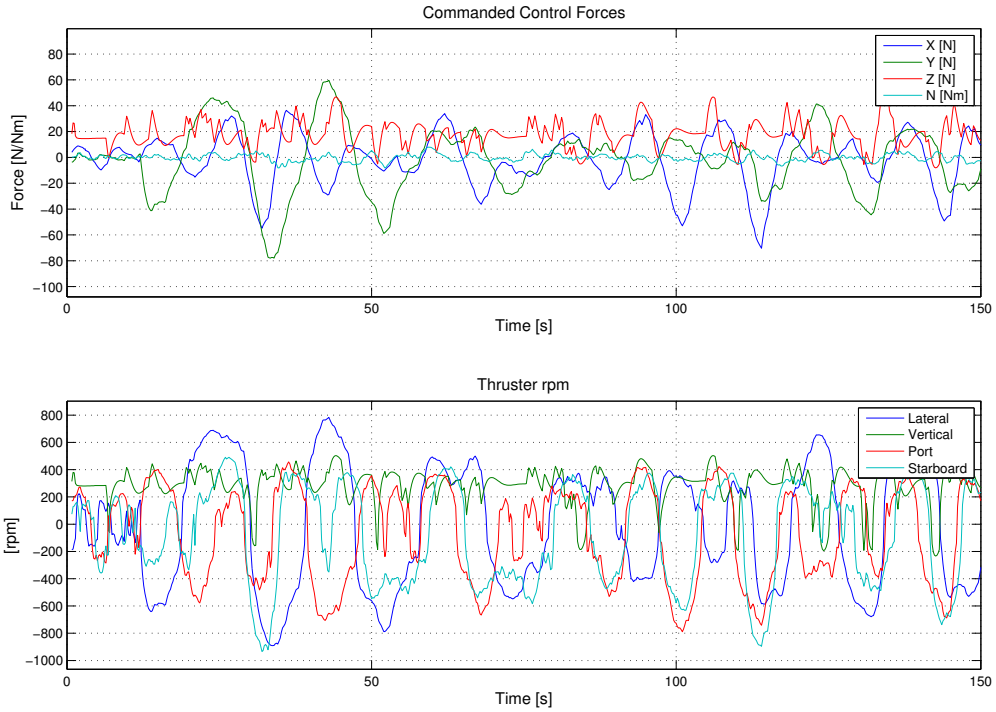

Figure 9.7: Full scale test: Dynamic positioning. Commanded thrust.

As seen in Figure 9.7, the thrust demands are varying in coherence with the oscillating deviation of position and heading. The maximum thrust for all the thrusters is around 1450 rpm in both directions. The lateral thruster, which is the most active thruster in this scenario, has a thruster demand that peaks at approximately 800 rpm, which is a little more than half of the maximum thruster effect. The reason for this is because the heading deviations is relatively large. As presented in Dukan [2011], the performance of the Fluxgate Compass on the ROV may degrade performance of the control system compared to when using a more precise instrument for the heading measurements, i.e. an IMU.

9.1.2 Performance Compared to Navipac

The performance of the control system using the implemented navigation system was also compared to the performance when using Navipac. The following plots, show the control system performance when switching between the implemented navigation system and Navipac. The control system is set to station keeping. The following scenario started off with navigation using the implemented navigation system. After about 25 seconds, the control system switched to using the data processed by Navipac. As can be seen on all the plots, the performance of the control system improved when using Navipac. Positioning in the north and east position, as shown in Figure 9.8 and 9.9, is improved from a deviation of approximate ± 0.4 m and ± 0.3 m respectively to below 10 cm in both positions. Although a similar improvement in heading is not so prominent in the raw signals, improvements can be seen in the estimation in Figure 9.11. Improvements in velocities and commanded thrust is also be seen in Figure 9.12 and 9.13. Using the Navipac for navigation reduces the strain on the thrusters from approximately 1000 rpm to 200 rpm in the most significant case.

The main reason for the difference in performance between the two navigation systems most likely lies in the delay of the signals in the communication between the navigation system and the control system. As shown in the previous chapter, the navigation system suffers from a signal delay of up to 0.6 seconds. This means that when the ROV actually is located in the desired position, the control system will think that the ROV is in the position that it *was* 0.6 seconds earlier. As a result, the control system will command the thrusters to drive the ROV 0.6 seconds longer than it should. This is most likely the cause of the larger deviation in all the states. The magnitude of the deviation will consequently be dependent on how the control system is tuned and the dynamic properties of the ROV. The implemented navigation system should however in the absence of the signal delay yield a more comparable performance compared to Navipac.

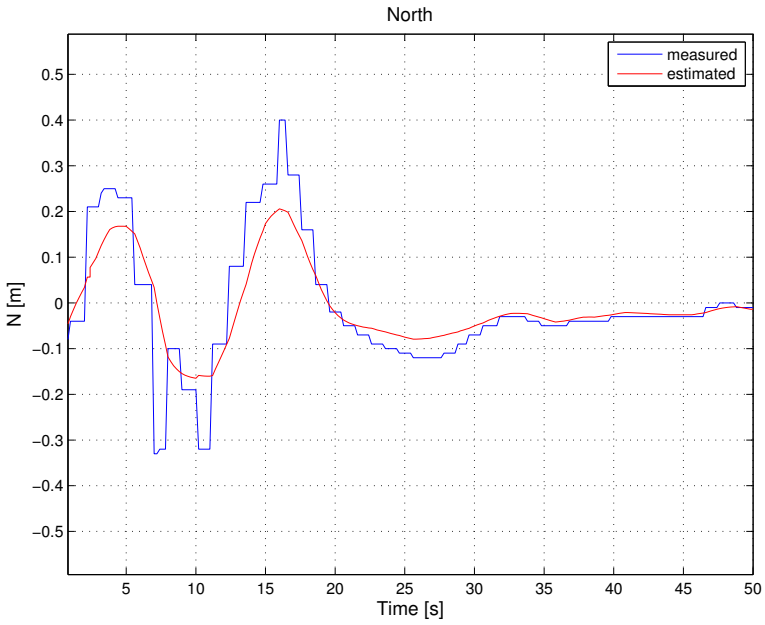

Figure 9.8: Full scale test: Switching between the navigation system and Navipac. North position.

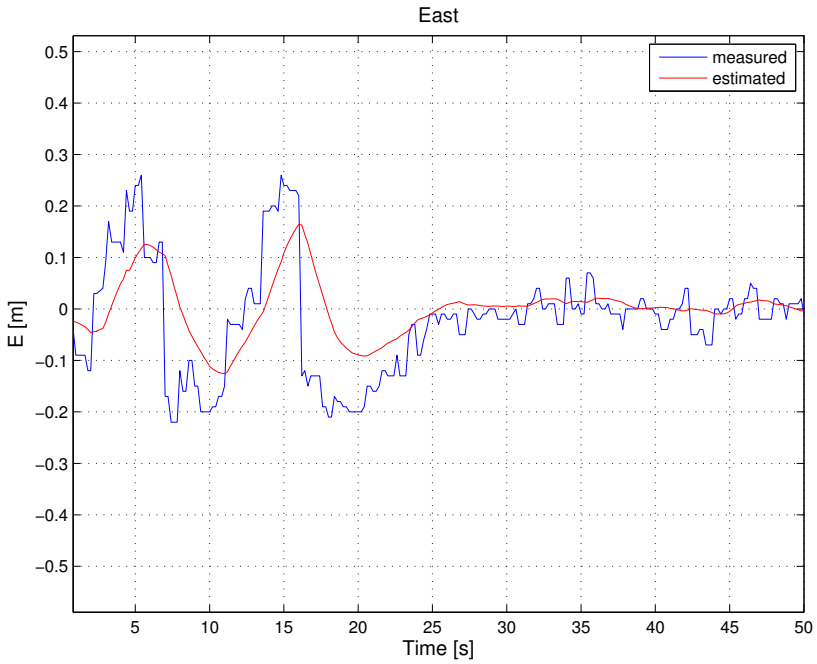

Figure 9.9: Full scale test: Switching between the navigation system and Navipac. East position.

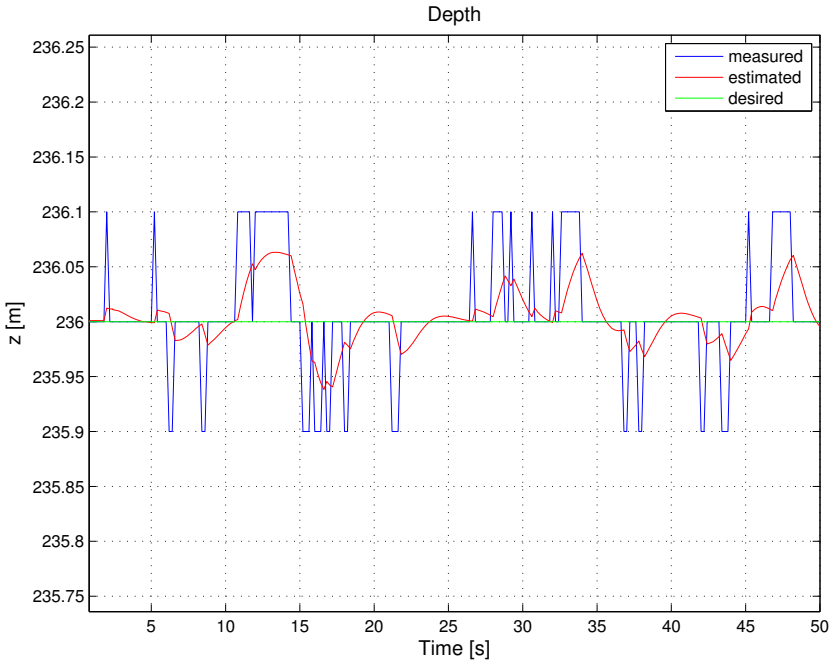

Figure 9.10: Full scale test: Switching between the navigation system and Navipac. Depth.

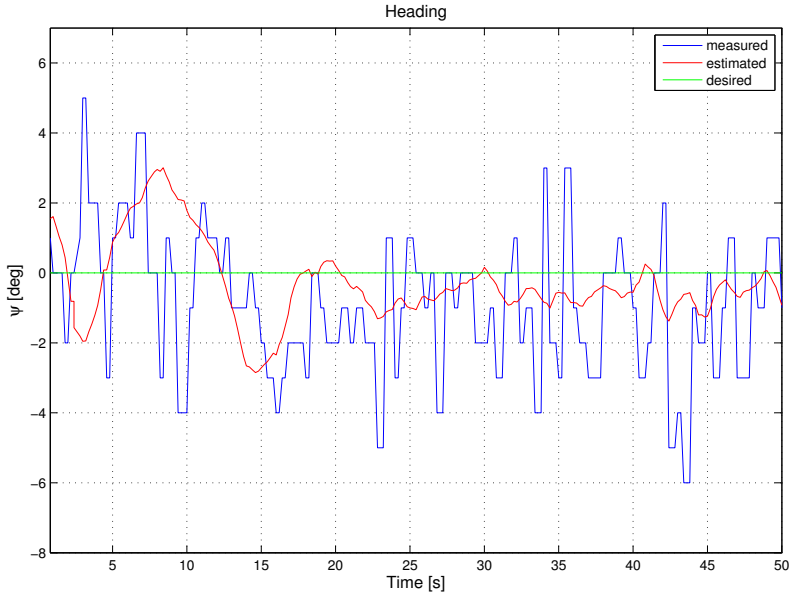

Figure 9.11: Full scale test: Switching between the navigation system and Navipac. Heading.

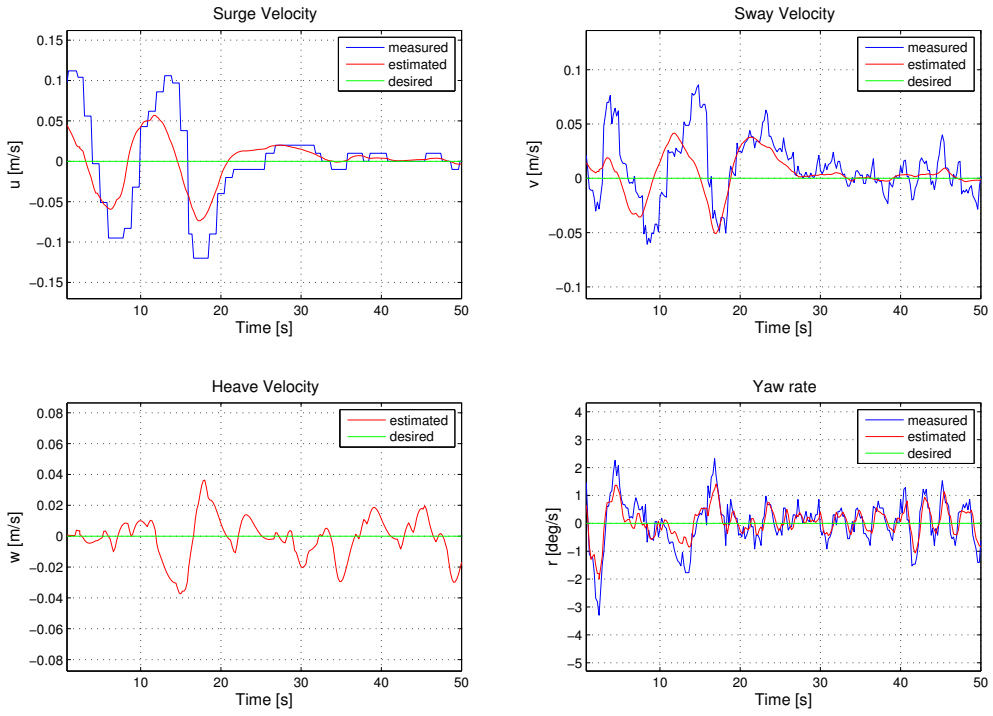

Figure 9.12: Full scale test: Switching between the navigation system and Navipac. Velocities.

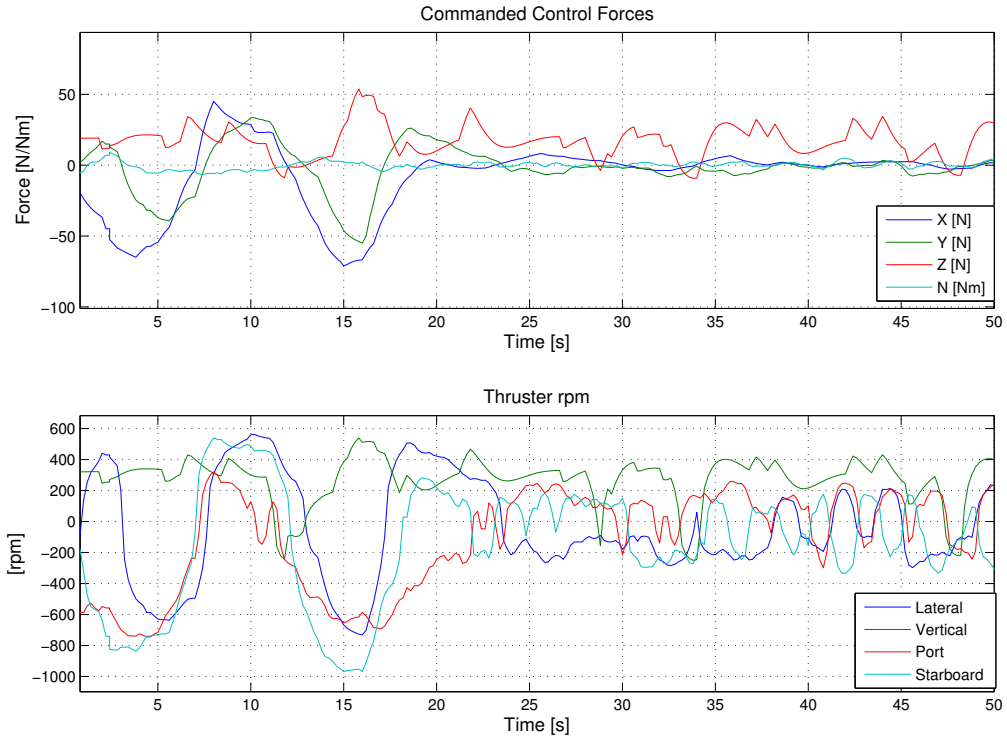

Figure 9.13: Full scale test: Switching between the navigation system and Navipac. Commanded thrust.

9.2 Moving Between Waypoints

A second test was also performed. The test shows that the control system is able to move the ROV between way points using the implemented navigation system with decent performance. The operation was to move the ROV 10 meters in the north position while east position, depth and heading were kept constant. As seen in Figure 9.14 and 9.15, the movement of the ROV took place between approximately 200 seconds and 260 seconds. Before and after the movement in north position, the states of the ROV is kept as pretty much the same values and deviation as in the station keeping test. This can be seen on all the different plots. During movement however, the east position and heading deviates more from the desired value than usual. The deviation in east position is roughly ± 1 m, while the deviation in the heading is between ± 15 degrees. The increased deviation in east position may be caused by the larger deviation in heading in the beginning of the movement, as seen in Figure 9.17 at around 200 seconds. Because the heading deviates so much in the beginning of the movement, the lateral thruster becomes more active in order to control the heading more aggressively, as shown in Figure 9.19.

Because the ROVs course is directly aligned with the north direction, the lateral thruster will directly affect the east position of the ROV. If the east position and the commanded lateral thrust is compared, Figure 9.15 and 9.19, it is evident that the peaks and the magnitude of the peaks correspond to each other. Positive rpm will here result in a negative east movement.

Another thing that is worth to notice is the demanded thrust during station keeping compared to when in movement. The commanded thrust during station keeping is surprisingly high compared to when the ROV is moving. This demonstrates how much strain the signal delay of the implemented navigation system is putting on the thrusters of the ROV.

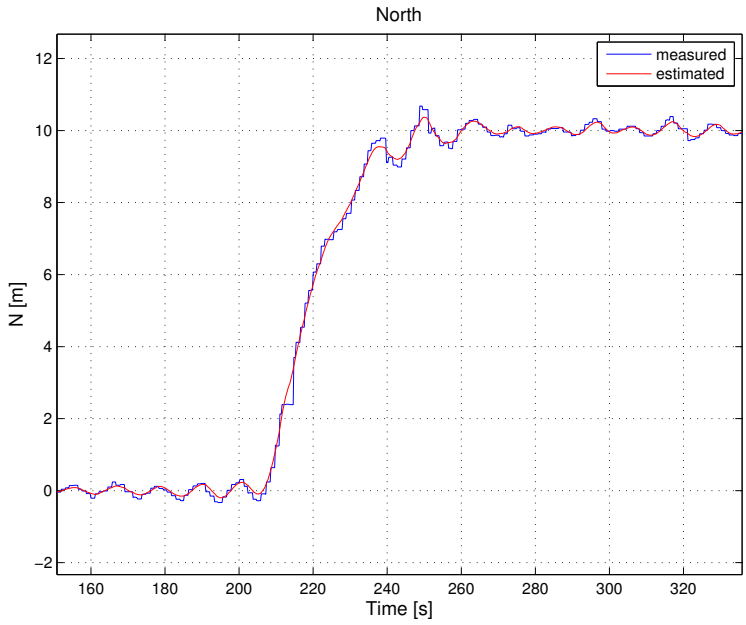

Figure 9.14: Full scale test: Moving between wayponts. North position.

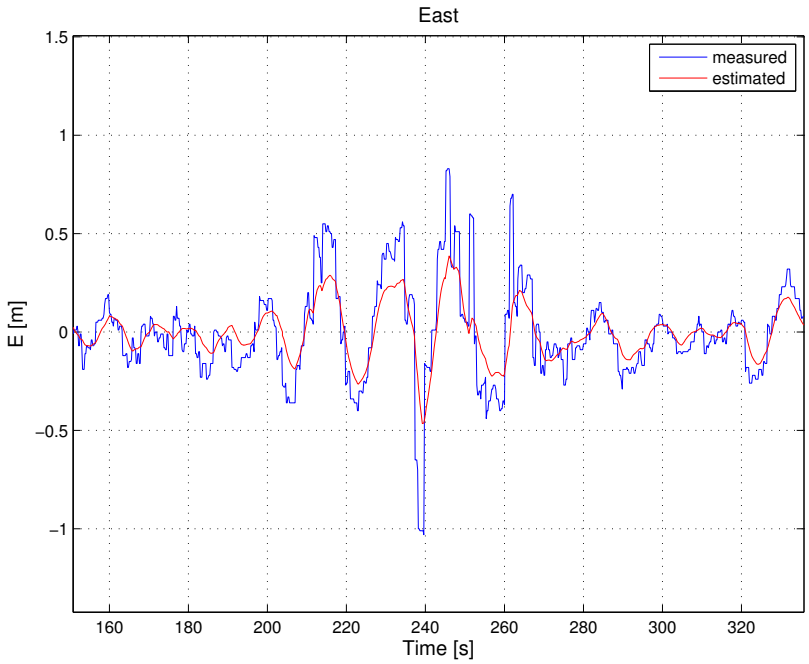

Figure 9.15: Full scale test: Moving between wayponts. East position.

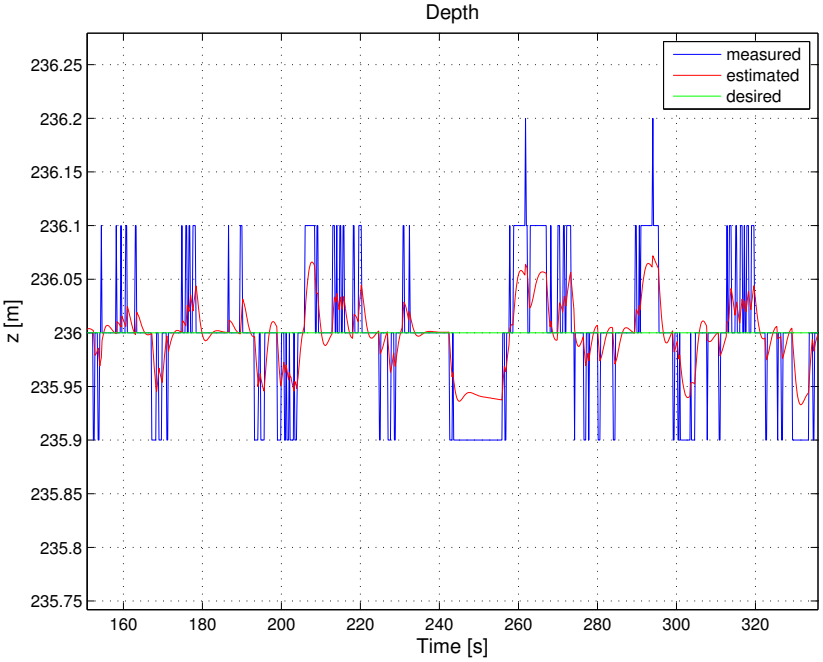

Figure 9.16: Full scale test: Moving between wayponts. Depth.

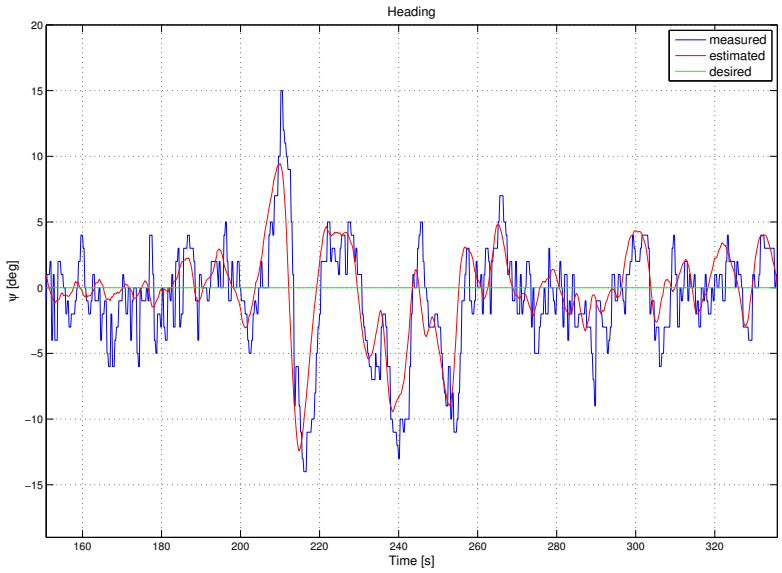

Figure 9.17: Full scale test: Moving between wayponts. Heading.

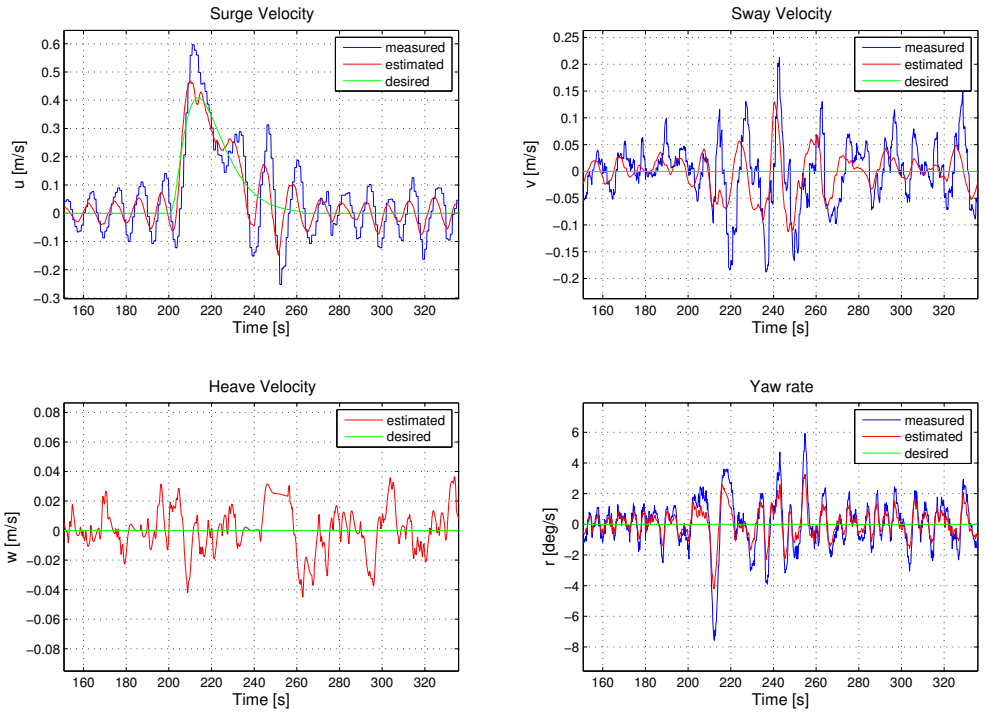

Figure 9.18: Full scale test: Moving between wayponts. Velocities and yaw rate.

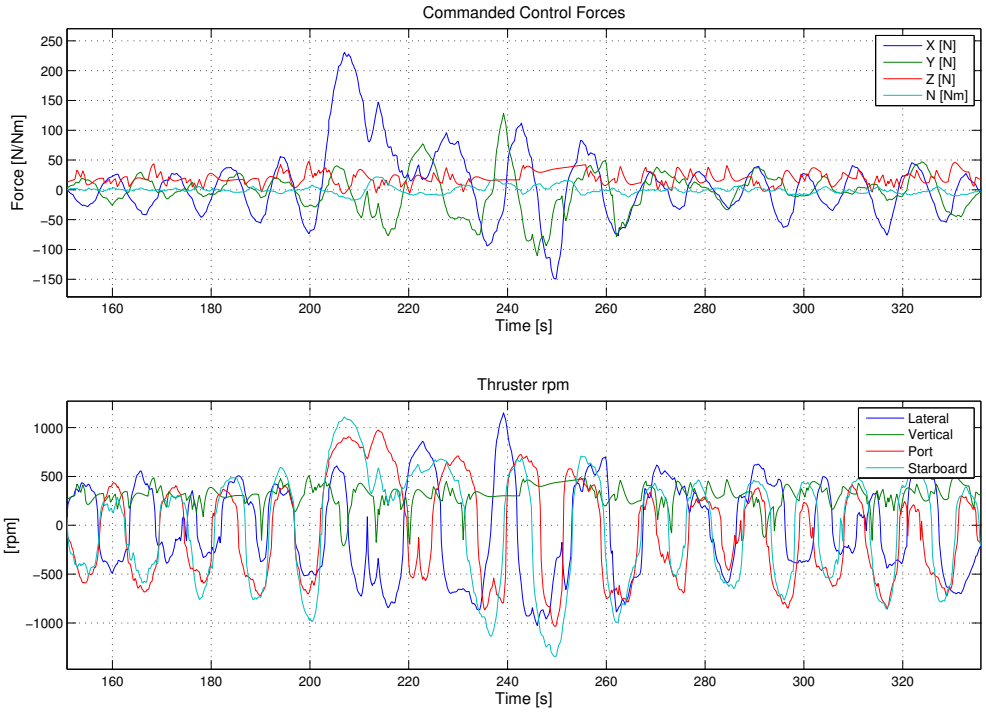

Figure 9.19: Full scale test: Moving between wayponts. Commanded thrust.

Chapter 10

Conclusion and Further Work

10.1 Conclusion

The results from full scale testing of the navigation system shows that the control system is able to perform station keeping and way point maneuvering operations using the navigation system that has been developed. However, compared to navigation using Navipac, the performance of the control system is somewhat degraded. Station keeping deviations go from ± 0.4 m to ± 0.1 m when switching from navigation using the developed navigation system to navigation using Navipac. A delay in the communication between the navigation system and the control system in the magnitude of either 2 or 3 control system loop iterations (400 ms-600 ms), may be the cause of the performance degradation.

Comparing the kinematic calculations of the ROV position, using methods presented in the theory of this thesis, with the ROV position calculated by Navipac shows a small deviation in the magnitude of 0.4 m in the east position and 0.1 m in the north position. The source causing this difference cannot be identified by the tests that were performed. Additional testing must be done to verify if the difference is caused by inaccurate sensor offsets or not. It is also hard to conclude which of the two positions that is closest to the true position of the ROV in the local reference frame without performing tests with fixed transponders in known positions.

Overall, a functional navigation system that is capable of performing simple operations of the ROV has been developed during the course of this thesis. A starting point has been made for further development of the navigation system and is available for future students who wishes to pursue the task. Some suggestions for further work will be made in the following.

10.2 Suggestions for Further Work

The most important thing to investigate further is the cause of the performance degradation when compared to Navipac. In particular, the delay in communication between the navigation system and the control system should be solved. One possible solution could be to change the communication setup between the Compact RIO hardware of both the control system and the navigation system and their respective host PCs. All the devices can be connected to the same switch and communication

between the the navigation system and the control system can be done us TCP/IP protocols as opposed to serial port communication.

Efforts should also be made to calibrate and identify the real sensor offsets and also verify the ROV position calculations. This can be done if the AUR lab has a fixed transponder in a known location at disposal.

Signal processing of the raw sensor signal should also be incorporated into the system in the future. Some of the sensors, especially the HiPAP, will from time to time suffer from degraded performance due to external conditions. This can sometimes greatly affect the performance of the control system. Signal processing algorithms that optimize the performance of the control system in these conditions will be of great value.

The Kalman filter that has been implemented should also be revised to include dead reckoning capabilities and state estimation to increase redundancy. If an IMU is added in to the sensors arsenal of the ROV Minerva in the future, the filter should be made so that additional states are easily added. In the case of adding an Motion Reference Unit (MRU) to the ROV Minerva, the development of hydroacoustic aided inertial navigation system should be pursued.

User friendliness of the system should also be considered. If the navigation system someday will serve as a backup for Navipac, users with a non technical background may want to use the system, i.e. during biological surveys. Also, NMEA navigational sentences should be supported in a more general form (perhaps in the form of a database?) to make addition of sensors more easy for a person without detailed insight in the navigation program. By doing this, the navigation system will also be more easily adapted to navigation of other ROVs that perhaps has a different sensor configuration.

The plotting of the ROV and vessel position could also be extended to include real map data where the positions are plotted on a map projection in order to visualize the navigation in a more practical manner. The National Instruments developer community has some good examples where map data from Google is imported into Labview.

References

Andreas Antoniou. *Digital Signal Processing*. McGraw Hill, 2005.

Steve Beiter, Ray Poquette, Bill San Filipo, and Walter Goetz. Precision hybrid navigation system for varied marine applications, 1998.

Robert Grover Brown and Patrick Y C Hwang. *Introduction to Random Signals and Applied Kalman Filtering*. Wiley, 1997.

Creative Commons. Galileo. http://en.wikipedia.org/wiki/Galileo_satellite_navigation, 2011.

Fredrik Dukan. Dynamic positioning system for a small size rov with experimental results. Technical report, NTNU, 2011.

Steven Dutch. Converting utm to latitude and longitude (or vice versa). http://www.uwgb.edu/dutchs/usefuldata/utmformulas.htm, 2011.

Federal Space Agency. GLONASS Information Analytical Centre. , 2010.

Borje Forssell. *Radio Navigation Systems*. Prentice Hall International, 1991.

Thor I. Fossen. *Guidance and Control of Marine Craft*. Norwegian University of Science and Technology, 2010.

Kenneth Gade. Navlab, a generic simulation and post-processing tool for navigation. *European Journal of Navigation*, 2(4), November 2004.

Teledyne RD Instruments. *Acoustic Doppler Current Profiler Principles of Operation A Practical Primer*, 2006.

Teledyne RD Instruments. Teledyne rd instruments navigation product. http://www.rdinstruments.com/nav_main.aspx, 2011.

Bjørn Jalving, Kenneth Gade, Ove Kent Hagen, and Karstein Vestgård. A toolbox of aiding techniques for the hugin auv integrated inertial navigation system, 2004.

Christopher Jekeli. *Inertial Navigation Systems with Geodetic Applications*. deGruyter, 2001.

Norvald Kjerstad. *Elektroniske og Akustiske Navigasjonssystemer*. Tapir Akademiske Forlag, 2010.

Glenn Nolan Kristin E. Gribble and Donald M. Anderson. Biodiversity, biogeography and potential trophic impact of protoperidinium spp. (dinophyceae) off the southwestern coast of ireland. *JOURNAL OF PLANKTON RESEARCH*, 29(11), 2007.

Kongsberg Maritime. Technical specifications for the hipap family. http://www.km.kongsberg.com/, 2011.

NTNU. Minerva Home Page. http://www.ntnu.edu/marine/facilities, 2010.

Darrel Turkington. *Matrix Calculus and Zero-One Matrices*. Cambridge University Press, 2002.

Greg Welch and Gary Bishop. An introduction to the kalman filter. *Automatica*, 2001.